



# 1 Review Article: Permafrost Trapped Natural Gas in 2 Svalbard, Norway

3 Authors: Thomas Birchall\*<sup>1,2</sup>, Malte Jochmann<sup>1,3</sup>, Peter Betlem<sup>1,2</sup>, Kim Senger<sup>1</sup>, Andrew  
4 Hodson<sup>1</sup>, Snorre Olaussen<sup>1</sup>

5 <sup>1</sup>Department of Arctic Geology, The University Centre in Svalbard, P.O. Box 156, N-9171 Longyearbyen,  
6 Svalbard, Norway

7 <sup>2</sup>Department of Geosciences, University of Oslo, P.O. Box 1047, Blindern, 0316 Oslo, Norway

8 <sup>3</sup>Store Norske Spitsbergen Kulkompani AS, Vei 610 2, 9170 Longyearbyen, Svalbard, Norway

9 \*Correspondence to: Thomas Birchall ([Thomas.birchall@unis.no](mailto:Thomas.birchall@unis.no))

10

11 **Abstract.** Permafrost has become an increasingly important subject in the High Arctic archipelago of Svalbard.  
12 **However,** whilst the uppermost permafrost intervals have been well studied, the processes at its base and the  
13 impacts of the underlying geology have been largely overlooked. More than a century of coal, hydrocarbon and  
14 scientific drilling through the permafrost interval shows that accumulations of natural gas trapped at the base  
15 permafrost is common. They exist throughout Svalbard in several stratigraphic intervals and show both  
16 thermogenic and biogenic origins. These accumulations combined with the relatively young permafrost age  
17 indicate gas migration, driven by isostatic rebound, is presently ongoing throughout Svalbard. The accumulation  
18 sizes are uncertain, but one case demonstrably produced several million cubic metres of gas over eight years. Gas  
19 encountered in two boreholes on the island of Hopen appears to be situated in the gas hydrate stability zone and  
20 thusly extremely voluminous. While permafrost is demonstrably ice-saturated and acting as seal to gas in  
21 lowland areas, in the highlands it appears to be more complex, and often dry and permeable. Svalbard shares a  
22 similar geological and glacial history with much of the Circum-Arctic meaning that sub-permafrost gas  
23 accumulations are regionally common. With permafrost thawing in arctic regions, there is a risk that the impacts  
24 of releasing of sub-permafrost trapped methane is largely overlooked when assessing positive climatic feedback  
25 effects.

26

## 27 **Keywords**

28 Permafrost; Top seal; Natural Gas; Cryosphere; Greenhouse Gas; Arctic; Greenhouse Gas; Hydrates.

29



## 30 1 Introduction

31 It is generally accepted that thawing permafrost results in the release of methane gas to the atmosphere  
32 (Knoblauch et al., 2018). Methane is a potent greenhouse gas and its release from permafrost acts as a positive  
33 climatic feedback loop (Boucher et al., 2009; Howarth et al., 2011; Lashof and Ahuja, 1990). The Arctic is  
34 particularly sensitive to climatic changes and Svalbard is even more so due to the West Spitsbergen Current  
35 (Divine and Dick, 2006; Van Pelt et al., 2016; Aagaard et al., 1987). Svalbard is, therefore, a critical site for  
36 studying the evolution of permafrost and sub-permafrost processes (Hornum et al., 2020; Hodson et al., 2019;  
37 Christiansen et al., 2010; Isaksen et al., 2000).

38 While methane emissions from thawing of the permafrost active layer is relatively well understood (Knoblauch  
39 et al., 2018; Vonk and Gustafsson, 2013), the prevalence and volumes of gas accumulations trapped beneath the  
40 permafrost “cryospheric cap” (Anthony et al., 2012) has been much less studied. Here we present evidence of  
41 such gas accumulations in Svalbard, where the relatively young permafrost (Gilbert et al., 2018) appears to be  
42 regionally sealing significant gas accumulations. The gas here may originate from biogenic or thermogenic  
43 processes (Hodson et al., 2019; Ohm et al., 2019) and may be in free-form or, under the right compositional and  
44 thermobaric conditions, in the form of natural gas hydrates (Sloan Jr et al., 2007; Betlem et al., 2019).

45 Occurrences of gas originating from within or below intervals of permafrost are typically identified in studies on  
46 natural gas hydrates and have been documented in both the Russian (Chuvilin et al., 2000; Makogon and  
47 Omelchenko, 2013; Yakushev and Chuvilin, 2000; Skorobogatov et al., 1998; Chuvilin et al., 2020) and North  
48 American Arctic (Bily and Dick, 1974; Collett et al., 2011; Kamath et al., 1987; Majorowicz and Hannigan,  
49 2000; Nielsen et al., 2014).

50 Permafrost is defined as ground that remains at sub-zero (in Celsius) temperature for more than two consecutive  
51 years, regardless of fluid content. Physically speaking, ice-saturated permafrost possesses extremely good sealing  
52 properties (Keating et al., 2018). However, how effective it is as a top seal is uncertain, this is reflected in  
53 Svalbard by methane emissions at pingos (Hodson et al., 2019) where permafrost demonstrates its local sealing  
54 ability but also the prevalence of migration pathways through it. Abrupt changes in hydrogeological flow  
55 conditions at the base of permafrost also indicate the permeability-reducing nature of the permafrost interval  
56 (Hornum et al., 2020). In geological terms, permafrost is very short-lived which, in addition to being very  
57 shallow and potentially patchy, would typically preclude it from being regarded as a feasible seal for  
58 conventional hydrocarbon accumulations at geological time-scales of millions of years.

59 In Svalbard, methane migrating through near-coastal pingos shows characteristics of a biogenic origin (Hodson  
60 et al., 2019). Approximately three kilometres inland, analysis of gas encountered at the base of permafrost during  
61 drilling indicated a further contribution from thermogenic origins (Ohm et al., 2019). Several hydrocarbon source  
62 rocks are encountered in Svalbard, so traces of thermogenic gas are not particularly surprising. What is  
63 surprising, and the focus of this study, is the widespread occurrence, both spatially and stratigraphically, of gas  
64 accumulations at the base of permafrost in Svalbard. In this contribution, we therefore provide previously  
65 unpublished data from 41 boreholes to provide a systematic review of the occurrence of sub-permafrost gas



66 accumulations from Svalbard. We also analyse data from these boreholes to attempt to characterise the  
67 permafrost, its thickness and sealing properties.

## 68 2 Geological and physiographic setting

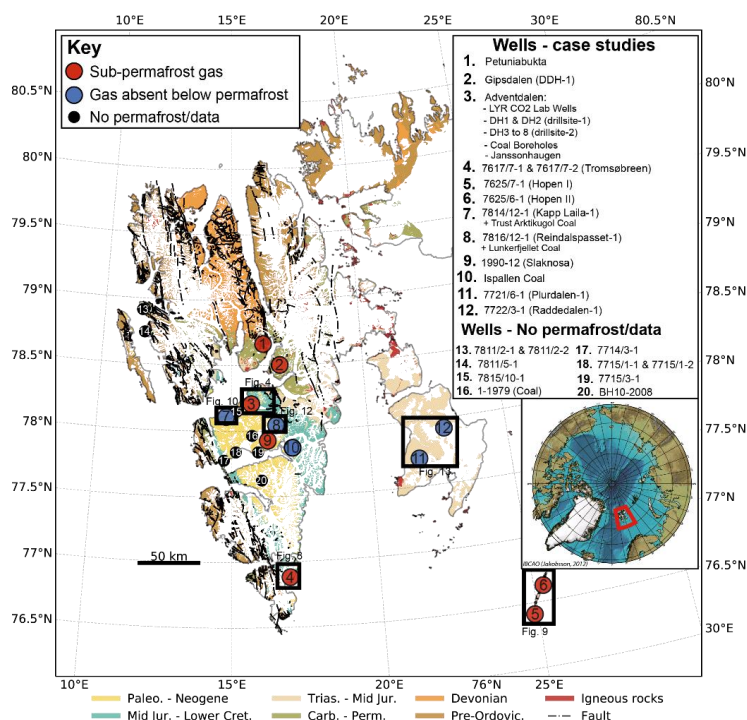
69 The Svalbard archipelago is situated in the high arctic between 74° to 81°N and 15° to 35°E with sub-zero  
70 average temperatures for eight months of the year. Despite this, due to repeated glaciations and the warming  
71 effects of the West Spitsbergen Current, permafrost in Svalbard is not as thick as some other pan-arctic regions  
72 (Humlum, 2005).

73 Permafrost in Svalbard ranges in thickness from more than 500 m in mountainous areas inland and thins to less  
74 than 100 m near the coastlines (Humlum, 2005). Continuous sub-sea permafrost has not been shown to exist  
75 offshore on Spitsbergen's west coast (Christiansen et al., 2010) and is not believed to be present offshore  
76 elsewhere around Svalbard (Humlum et al., 2003; Landvik et al., 1988), although these areas have been little  
77 studied in this respect and may feature locally discontinuous permafrost. Because of the West Spitsbergen  
78 Current, temperatures are much warmer on the west coast than the east. Although poorly studied in eastern parts,  
79 one can reasonably anticipate thicker permafrost due to colder temperatures, as is also shown by numerical  
80 modelling of the permafrost-associated gas hydrate stability zone (Betlem et al., 2019). However, thicker  
81 insulating snow coverage in coastal settings can also help in preventing winter heat loss from the ground and  
82 limit permafrost growth (Humlum et al., 2003). In a more local context, permafrost in Adventdalen has been  
83 relatively well studied with near-zero thickness on the coast rapidly thickening to approximately 150 m thick 3  
84 km inland at the Longyearbyen CO<sub>2</sub> site and approximately 220 m thick in the valley at Janssonhaugen, some  
85 fifteen kilometres from the coast (Isaksen et al., 2000; Harada and Yoshikawa, 1996; Gilbert et al., 2018).

86 The permafrost history of Svalbard is something of a contentious issue but it is important to understand as it  
87 provides clues to the timing and rate of gas accumulation at its base. The driver for the permafrost evolution in  
88 Svalbard is dependent on glacial settings rather than temperature changes. During the Weichselian glacial stage  
89 (115 kya to 11.7 kya) Svalbard was covered by thick glacial ice, although the extent and thickness of this ice  
90 cover is still debated (e.g. Gataullin et al., 2001; Lambeck, 1996; Winsborrow et al., 2010). Glacial striations in  
91 several locations suggest that these glaciers were warm-based for at least parts of the Weichselian glaciation  
92 (Humlum, 2005; Humlum et al., 2003). The frictional heat generated from the sliding of warm-based glaciers  
93 likely thawed permafrost in major valleys (Humlum et al., 2003). Sedimentological and cryostratigraphic  
94 analysis of boreholes in Adventdalen support this (Gilbert et al., 2018), suggesting permafrost here has formed in  
95 the past few thousand years following the dynamic retreat of these warm-based glaciers and ice streams. Whether  
96 permafrost survived the Weichselian glaciations is dependent on the persistence of ice-free zones and/or cold  
97 based glaciers. Because of this, permafrost in highland areas was more likely to have survived, possibly for  
98 several hundred thousand years, through multiple glacial events (Humlum et al., 2003). There is also strong  
99 evidence of lowland areas in north-western Svalbard being ice-free at this time which may have enabled the  
100 persistence of much older permafrost (Landvik et al., 2003). Valley settings are pertinent to this study as the  
101 majority of wellbores have been drilled in valleys or near to the coast for logistical reasons.



102 **Per**mafrost often poses a challenge to geologists, particularly for drilling boreholes (Vrielink et al., 2008), and  
 103 acquiring and processing seismic data (Schmitt et al., 2005; Johansen et al., 2003). This is because it changes the  
 104 properties of shallow unlithified sediments to become much more rigid and cemented by ice. Therefore, the  
 105 permafrost interval has much faster seismic velocities and can lose mechanical competence as it is drilled  
 106 through with heated or saline fluids. The near-surface rocks in Svalbard are typically well cemented and very  
 107 rigid due to deep burial and subsequent uplift.



108

109 **Figure 1** – Map of Svalbard with boreholes and areas of interest investigated in this study. Geological data is courtesy  
 110 of Norwegian Polar Institute (Dallmann et al, 2015). The locations of maps shown in later figures are highlighted.

111 In a tectonic context, Svalbard represents the exposed north-western part of the Norwegian Barents Sea  
 112 continental shelf. Other than the upper Cretaceous and parts of the Neogene, Svalbard exhibits a continuous  
 113 stratigraphic record from the Devonian to present (Steel and Worsley, 1984). Figure 1 shows the distribution and  
 114 ages of outcrops in Svalbard and the key wellbore sites for this study. Palaeozoic events from the Caledonian  
 115 (Gasser, 2014) and Ellesmerian-Svalbardian (Piepjohn, 2000) orogenies are predominantly recorded in the  
 116 remote northern parts of Svalbard. From the Late Carboniferous to Permian, mixed shallow marine rocks were  
 117 deposited in local basins (Smyrak-Sikora et al., 2019; Bælum and Braathen, 2012). From the Triassic to Early  
 118 Cretaceous, clastic deposition occurred in regional-scale basins (Steel and Worsley, 1984). The drainage pattern  
 119 changed from the west in the Early Triassic to the east from the Middle Triassic. During this time Svalbard sat  
 120 on the peripheries of the largest recorded delta system in Earth's history (Anell et al., 2014; Klausen et al., 2019;



121 Mørk, 2013). The latest Triassic to middle Jurassic saw much less sedimentation with numerous hiatuses and  
122 changes in drainage (Olaussen et al., 2018; Rismyhr et al., 2019). The late Jurassic to early Cretaceous saw  
123 greater deposition, including regionally important source rock intervals, and change in drainage due to the  
124 opening of the Amerasian Basin (Dypvik and Zakharov, 2012; Koevoets et al., 2018). During the Early  
125 Cretaceous the development of the High Arctic Large Igneous Province is evident from predominantly mafic  
126 dykes and sills in Svalbard (Senger et al., 2014). This likely resulted in major erosion during the late Cretaceous  
127 and early Palaeocene (Jochmann et al., 2019).

128 In Svalbard and the rest of the Barents Shelf, the Cenozoic geological history is the most important to understand  
129 subsurface fluid flow. In Svalbard, the Eocene was the time of maximum burial (Dörr et al., 2018), while in  
130 much of the Barents Sea maximum burial and hydrocarbon generation was probably during the late Oligocene to  
131 early Miocene (Henriksen et al., 2011; Faleide et al., 1996). From the Eocene to present major regional uplift of  
132 1 to 3 km has occurred and is ongoing with Svalbard experiencing the greatest uplift magnitudes, hence being  
133 subaerially exposed (Dimakis et al., 1998; Lasabuda et al., 2018). For this study, the most pertinent tectonic  
134 events are of widespread uplift and erosion due to repeated glacial cycles of the past few million years (Dimakis  
135 et al., 1998; Landvik et al., 1998). These recent events are still ongoing, and are the most important with respect  
136 to the migration and leakage of hydrocarbons from deeper traps to the shallow subsurface (Ohm et al., 2008;  
137 Abay et al., 2017).

138 The prevalence of hydrocarbon shows and gas influxes throughout the stratigraphy can be attributed to the  
139 presence of multiple mature source rocks (Ohm et al., 2019). The marine shales of the Jurassic Agardhfjellet  
140 Formation of the Adventdalen Group and the Triassic Botneheia Formation of the Sassendalen Group are both  
141 regionally extensive and prolific source rocks, responsible for charging the majority of the oil and gas  
142 discoveries in the Norwegian Barents Sea. In addition, organic-rich shales in the Gipsdalen Group (Braathen et  
143 al., 2012) probably represent laterally restricted source rocks. Carboniferous, Cretaceous and Paleogene coal  
144 seams have been exploited in Svalbard's past, with the latter still being produced in the Central Tertiary Basin in  
145 Adventdalen and Barentsburg. These coal seams are widespread and are typically gas-prone and oil-prone source  
146 rocks (Marshall et al., 2015; Uguna et al., 2017).

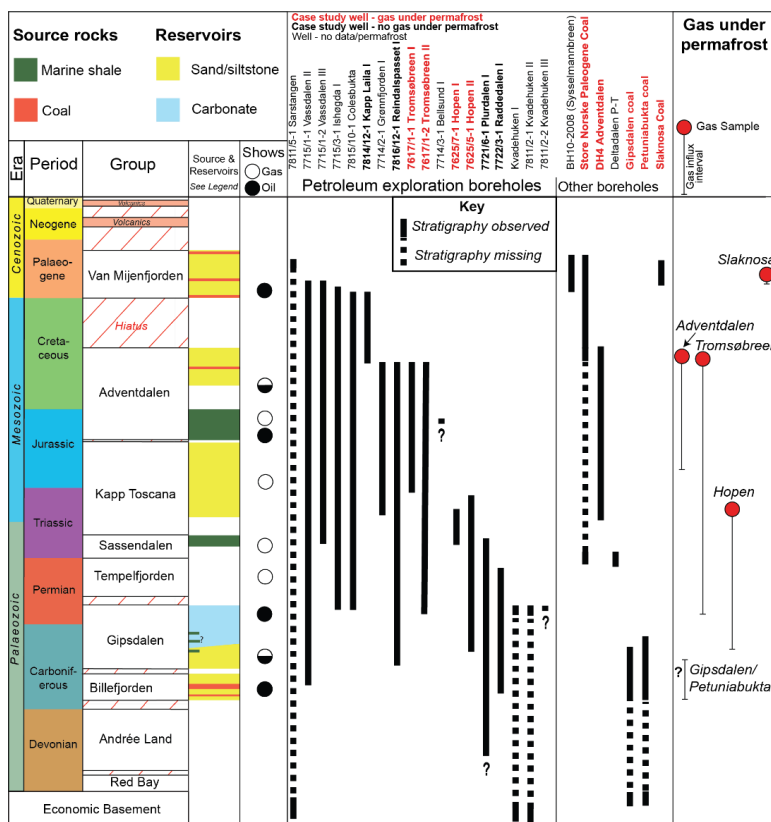
147 Numerous sandstones and karstified carbonates provide potential reservoirs throughout Svalbard's stratigraphy,  
148 many of which are direct analogues to proven hydrocarbon reservoirs in the Barents Sea (Nøttvedt et al., 1993).  
149 For this study the most notable reservoirs are the shallow marine sandstone-dominated Lower Cretaceous  
150 Helvetiafjellet and Carolinefjellet Formations (Steel et al., 1981; Grundvåg et al., 2019), and the Triassic-Jurassic  
151 Kapp Toscana Group deltaic to shoreline deposited siltstone and sandstones (Mørk, 1999).

152 The above-mentioned source rocks are also the best candidates for sealing intervals. In addition, the mudstones  
153 of the late Palaeocene Basilika Formation and Palaeocene-Eocene Frysjaodden Formation also possess potential  
154 sealing properties (Steel et al., 1981). The numerous source rocks, technical oil and gas discoveries, bitumen  
155 stained strata and surface seeps suggest that Svalbard possesses working petroleum systems, though none of the  
156 eighteen exploration wells drilled onshore Svalbard from 1961 to 1994 resulted in commercially viable  
157 discoveries (Senger et al., 2019). Although hydrocarbon accumulations likely first formed tens of millions of



158 years ago when source rocks were at maximum burial (Magoon and Dow, 2000), subsequent tectonic events  
 159 have undoubtedly caused tertiary fluid migration (Abay et al., 2017; Ohm et al., 2008).

160 The most recent deglaciation of the Barents Ice Sheet from 15 to 10 kya probably caused tilting and hydrocarbon  
 161 spillage from existing traps, furthermore glacial and overburden unloading resulted in remigration. Gas,  
 162 particularly methane, is the dominant hydrocarbon found in Svalbard due to the prevalence of over-mature or  
 163 gas-prone source rocks (Michelsen and Khorasani, 1991; Ohm et al., 2019; Senger et al., 2019) and active  
 164 methanogenesis (Hodson et al., 2019). Deglaciation and uplift has reduced confining pressure on subsurface  
 165 fluids and led to gas exsolution and expansion. Therefore, the subsurface fluid systems in Svalbard are in a state  
 166 of disequilibrium and widespread hydrocarbon migration is likely ongoing at present (Abay et al., 2017).  
 167 Evidence of this is manifested as out-of-equilibrium pore pressures (Birchall et al., 2020) and the previously  
 168 mentioned surface seeps.



169

170 **Figure 2 – The hydrocarbon exploration wells of Svalbard and key coal and scientific boreholes showing the**  
 171 **stratigraphy they penetrated, modified from Senger et al. (2019). The base-permafrost, gas-bearing stratigraphy is**  
 172 **shown in the right hand column.**

173 In Svalbard, the timing of hydrocarbon migration and permafrost formation overlap, meaning there is potential  
 174 for accumulations to develop beneath the impermeable permafrost. Although numerous hydrocarbon and coal



175 exploration wellbores penetrate the entire permafrost interval, it has rarely been of interest to the operators  
176 (Senger et al., 2019). However, on detailed inspection of well data, reports, and anecdotal evidence, it is clear  
177 that sub-permafrost gas accumulations have been frequently encountered throughout the archipelago. In  
178 Adventdalen, sub-permafrost free-gas was first documented in 1967 during coal exploration and encountered  
179 again in 1979 (Snsk, 1981). This accumulation was further confirmed, and sampled (Ohm et al., 2019; Huq et al.,  
180 2017), during scientific drilling of the Longyearbyen CO<sub>2</sub> Lab between 2008 and 2012. Figure 2 shows the key  
181 wellbores of this study, the stratigraphy they penetrate in Svalbard and whether they encountered gas at the base  
182 of permafrost, which is the main point of discussion in this contribution.

### 183 3 Data and methods

184 Several decades of coal and petroleum exploration, as well as research drilling, in Svalbard has led to much  
185 anecdotal evidence of gas accumulations beneath permafrost. We have attempted to verify this by analysing data  
186 from boreholes that have penetrated through the permafrost in Svalbard. These boreholes include eighteen  
187 hydrocarbon exploration wells, ten scientific boreholes, eight of which are from the Longyearbyen CO<sub>2</sub> Lab  
188 (from two drill sites). Also integral to this study are the somewhat sporadic data, including drilling and  
189 geological reports, from more than five hundred coal exploration boreholes drilled by the local Store Norske  
190 Spitsbergen Kulkompani (SNSK) over a period of nearly a century. We identify where gas accumulations occur  
191 and where these coincide with the base of permafrost, or the first permeable interval below it. One of the major  
192 challenges with these boreholes is that they typically target much deeper stratigraphy and often acquire very  
193 limited petrophysical data in the shallow parts. Typically, only the gamma ray logging tool, which measures the  
194 rocks natural radioactivity, is run in the shallow intervals. The available well data used in this study are presented  
195 in Table 1. Ascertaining the presence of sub-permafrost gas presents several challenges.

196 Identifying the presence of permafrost is simple and can often be clear from geomorphological features such as  
197 pingos. However, identifying the thickness and base of permafrost is much more challenging (Osterkamp and  
198 Payne, 1981). Table 2 shows the ideal responses of petrophysical and drilling data at the lower permafrost  
199 boundary and the challenges to each method. By far the biggest challenge to petrophysical and drilling data  
200 analysis in Svalbard is due to the low porosity, heterolithic, very rigid and overcompacted rocks (Henriksen et  
201 al., 2011). The nature of the base of permafrost itself is also not well understood, but it is a reasonable  
202 assumption that it is a diffuse boundary which adds to the complexity of identifying a permafrost boundary in  
203 petrophysical data alone. Further complications arise from the drilling fluid used and circulated in the wellbores  
204 which was often heated and hypersaline. Nevertheless, it is generally possible to identify the approximate base of  
205 permafrost on a case-by-case basis using all available data. Petrophysical data is robust in identifying lithology  
206 and drilling data is useful in identifying changes in fluid behaviour. When liquid water is encountered it is  
207 obvious evidence of being below the ice-bearing permafrost (though may be below 0°C, depending on salinity).  
208 Other indicators that can help identify the position of permafrost include ice-plug formation within the wellbore,  
209 sudden changes in the character or amount of drill cutting returns and increases in background gas  
210 measurements. The strongest indication of base permafrost occurs where fluid influxes into or out of the  
211 wellbore suddenly occur in thick, normally permeable sandstones. In this situation it is very likely it is due to the  
212 transition of impermeable permafrost to permeable water or gas-bearing rock. Abnormally high pressures at the



213 apparent base of permafrost are often mentioned in well reports and provide good evidence that the permafrost is  
 214 acting as an effective seal.

Petrophysics - Start of Data (m MD)						Gas Data				
Well	Gamma Ray	Resistivity	Acoustic	Density	Temperature	Cuttings	Gas Shows (Chromatograph)	Fluid Samples	Well Report	
Hydrocarbon Exploration										
7617/7-1 Tromsøbrecken-1	(Drilling parameters only)				BHT	Surface	Surface	768 m	Y	
7617/7-2 Tromsøbrecken-2	17	350	350	330	?	Surface	Surface	-	Y	
7625/7-1 Hopen-1	3.5	- (SP logged)	-	-	BHT	Surface	Surface	c. 150 m	Y	
7625/6-2 Hopen-2	Surface	349	349	638	Surface	Surface	Surface	-	Y	
7714/2-1 Grønnefjorden	not logged					Cored	-	-	Y	
7714/3-1 Bellsund	?								N	
7715/1-1 Vassdalen-2	Surface	17	-	-	-	-	-	-	N	
7715/1-2 Vassdalen-3	-									
7715/3-1 Ishøgda	Surface	Surface	Surface	Surface	Surface	Surface	-	-	N	
7721/6-1 Plurdalen	5	83	5	83	Surface	Surface	Surface	Water at 500 m	Y	
7722/3-1 Raddedalen	Surface	5	591	593	5	Surface	Surface	-	Y	
7811/2-1 Kvadehukenn-1	not logged					Cored	-	-	N	
7811/2-2 Kvadehukenn-2	not logged					Cored	-	-	N	
- Kvadehukenn-0	Shallow, no data									
7811/5-1 Sarstangen	30	615	-			BHT	Surface	260m	-	Y
7814/12-1 Kapp Laila	Surface	- (SP logged)	-			24 m (partial recovery)		-		Y
7815/10-1 Colesbukta	Surface	41	1467	-	-	-				
7816/12-1 Reindalspaset	From surface	22 (induction)	22	22	17.4	Surface	20 m	-	Y	
Selected Coal Boreholes										
1967-1 Adventdalen	Cored (not logged)					-		-	Y	



1979-10 Adventdalen							-	-	Y	
1979-11 Adventdalen							-	-	Y	
DDH1B Gippsdalen							-	-	Y	
1982-20	No data						-	-	1982 drilling summary	
Gruve 7 - H1							Y	-	1979 drilling summary	
1981-02							-	-	1981 drilling summary	
1981 (Platåberget)							-	-	1981 drilling summary	
1981-05 Breinosa							-	-	1981 drilling summary	
1981-06 Breinosa	Cored (not logged)						-	-	1981 drilling summary	
1979-1 Reindalen							-	-	Y	
1990-12 Slaknosa							-	-	Y	
Scientific Boreholes										
DH1	3	3	9	-	Surface	Cored	-	-	Y	
DH2	10	10	10	-	Surface	Cored	-	-	Y	
DH3	Cored: not logged						Cored	-	-	Y
DH4	Surface	440	440	-	Surface	Cored	-	Through out	Y	
DH5r	3	-	100	-	Surface	Cored	-	Below 645 m	Y	
DH6	Cored: not logged						Cored	-	Y	
DH7a	Cored: not logged						Cored	-	Below 645 m	Y
DH8 (Shallow)	Cored: not logged						Cored	-	-	Y
BH10-2008	Surface	67	48	Surface	-	-	-	-	Y	
Janssonhau- gen (temperature)	-	-	-		Surface	-	-	-	N	

215 Table 1 – Data availability and intervals recorded for the permafrost penetrating boreholes.



216 Direct temperature data from thermometers used in conjunction with wireline logging tools is common from  
 217 hydrocarbon exploration wells. However these were rarely allowed to reach thermal equilibrium with the  
 218 surrounding formations following drilling and fluid circulation. Therefore accurate absolute temperature  
 219 measurements are rare, though temperature trends (e.g. inflection points) can be used more qualitatively to  
 220 estimate base permafrost. Wells monitored over longer time periods, such as the scientific boreholes in  
 221 Adventdalen (Isaksen et al., 2000; Olaussen et al., 2019; Juliussen et al., 2010) are relatively rare, but provide  
 222 much more reliable and precise temperature data.

223 Identifying the presence of gas is relatively simple and, although petrophysical data is generally not helpful in  
 224 shallow sections for fluid discrimination. Reliable evidence comes from influxes of gas into the wellbore which  
 225 has been sampled from wells in Adventdalen, Tromsøbreen and Hopen (Senger et al., 2019). Elevated  
 226 background gas is another good indicator of sub-permafrost gas and is measured in drilling fluids returning to the  
 227 surface and extracted by a “gas trap”. This method typically identifies in-place dry gas accumulations or gas that  
 228 has exsolved from fluid on its way to the surface due to pressure decline. However, these measurements do not  
 229 detect gas that remains dissolved in formation water. Gas from drilling mud is also impacted by a variety of  
 230 factors (Marum et al., 2019), including drilling rate, drilling mud type and, perhaps the most pertinent,  
 231 temperature; low temperatures can cause heavier hydrocarbons to condense and avoid detection, it also causes  
 232 drilling fluids to become more viscous, further inhibiting gas extraction.

Log Type	Property Measured (Units)	Idealised Permafrost Response	Complicated by
<b>Petrophysical Data</b>			
<b>Gamma Ray</b>	Radioactivity of rocks (API)	No Response but useful in determining lithology.	N/A
<b>Acoustic (Sonic)</b>	Seismic velocity of rocks and fluids within. Measured in slowness (microsecond per foot)	Faster velocities (lower slowness) in icebound intervals.	Overcompacted, dense and rigid rocks. Low porosity and heterolithic rocks.
<b>Resistivity</b>	Resistivity of rocks and fluids within.	High resistivity in permafrost becoming low in water bearing interval.	Resistive hydrocarbons below permafrost. Fresh water below. Low porosity rocks. Clay rich and heterolithic rocks.
<b>Density</b>	Density of rocks and fluids within.	Decreased density in ice-bearing intervals	Low porosity. Heterolithic rocks (fluid response is generally overwhelmed by lithological response).
<b>Temperature</b>	Temperature of fluid in borehole at a given depth.	0°C or lower in permafrost interval.	Measures wellbore fluid, not fluid within formation. Drilling fluid circulates and is often heated. Requires a long time to equilibrate to formation.



<b>Fluid Sampling</b>	Pressure and fluid properties.	Qualitative - shows fluid phase and type. Abnormal pressures indicate a vertical barrier or seal.	Low permeability (including permafrost ice). Limited to few points in well. Shallow samples rarely of interest.
<b>Drilling Parameters</b>			
<b>Fluid Influx</b>	Fluid entering wellbore (often flowing to surface)	Indicates transition from impermeable to permeable zone.	Exact depth of influx is uncertain.
<b>Background Gas</b>	Measures levels and composition of gas returned with drilling fluid at the surface. Does not measure dissolved gas. (Percentage or parts per x)	Indicates transition from impermeable to permeable zone.	Varies depending on drilling rate, permeability, drilling mud type. Exact depth/formation of gas origin is uncertain.
<b>Rate of Penetration (ROP)</b>	The rate the drill bit penetrates the ground (ft. or m per hour)	A rapid rise in rate of penetration when transitioning from ice-bound to unbound rock. Best used with Weight-on-bit (1000 lbs) measurement.	Well-cemented, compacted and hard rocks. Rate can depend on external factors including drill bit condition.
<b>D-exponent</b>	Extrapolation of numerous drilling parameters to estimate pore-pressure.	May identify anomalously high drilling rate (or pressure) at base permafrost.	Well cemented, compacted and hard rocks. Heterolithic rocks. Largely qualitative.

233 **Table 2 – The petrophysical and drilling parameters that may identify permafrost and its base. Idealised responses**  
 234 **are shown and typically identify the transition from ice to water. The final column shows the complicating factors, all**  
 235 **of which are applicable to Svalbard. Perhaps the most pertinent complication to Svalbard is that the geology is**  
 236 **comprised of well cemented, compacted, hard rocks.**

237 In addition to well data, we also include data from published scientific studies including isotope (Huq et al.,  
 238 2017), thermobaric (Isaksen et al., 2000; Betlem et al., 2018; Betlem et al., 2019), geophysical (Beka et al.,  
 239 2017; Johansen et al., 2003) and geochemical (Leythaeuser et al., 1984; Ohm et al., 2008) analyses. We also  
 240 analysed Russian published literature for areas operated by Trust Arktikugol (Lyutkevich, 1937; Verba, 2013).

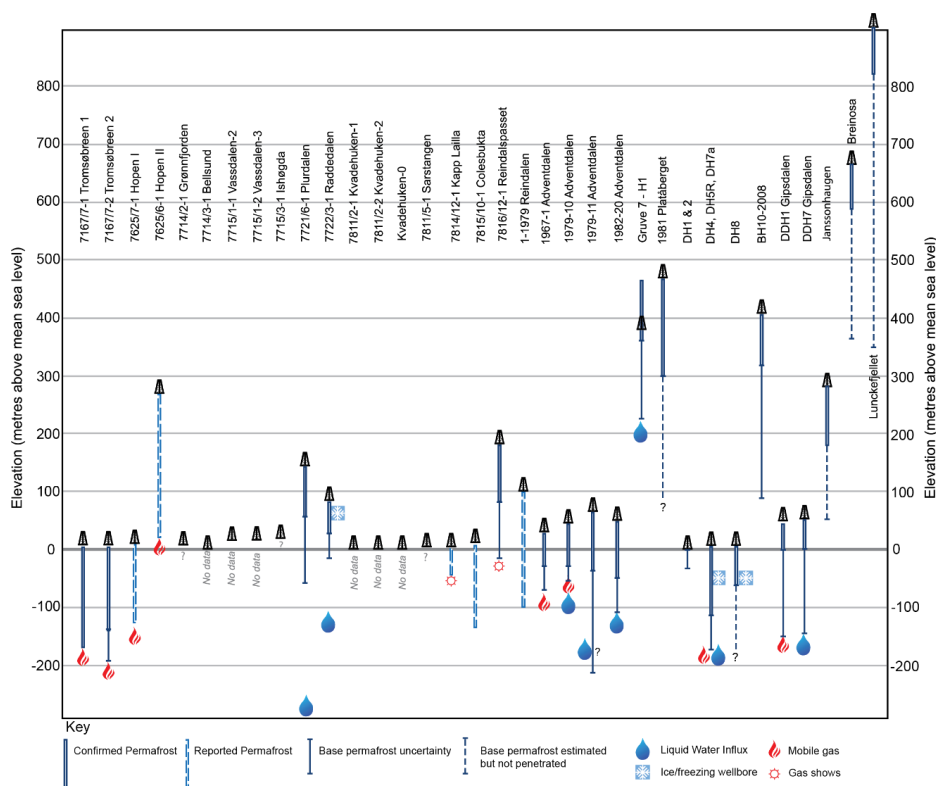
241 For Adventdalen, Tromsøbreen and Hopen we integrated all relevant data (summarised in Betlem et al., in  
 242 review; and references therein) in order to calculate the gas hydrate stability zone and permafrost extent for the  
 243 targeted study areas according to the workflow outlined in Betlem et al. (2019) and further refined in Betlem et  
 244 al. (in review). The workflow assumes steady-state conditions and implements structure-I gas hydrate phase  
 245 boundary curves generated through the  HYD modelling software (Masoudi and Tohidi, 2005).



246 **4 Results**

247 **4.1 Evidence of Permafrost**

248 Figure 3 shows which boreholes encounter permafrost, their elevation, and the depth to the base of permafrost.  
 249 Although it does not preclude its existence, there is no clear evidence of permafrost in the hydrocarbon  
 250 exploration wells on the west coast. On the shoreline of Isfjorden, the Kapp Laila and Adventdalen (DH1 and  
 251 DH2) wells show evidence of a thin permafrost interval, although it may not be ice-bearing. Wells on the east  
 252 coast of Spitsbergen at Tromsøbreen and on the southern beach of Hopen provide strong evidence of a thicker  
 253 permafrost top seal even in coastal locations. Wells further inland, including the majority of coal exploration  
 254 boreholes, unsurprisingly show evidence of thicker permafrost.



255  
 256 **Figure 3 - A plot of wells in this study showing their elevation and the depth to base permafrost. Solid well path**  
 257 **outlines show where data analysed in this study confirms the presence of permafrost while dashed outlines represent**  
 258 **where base permafrost has been reported but data is not available. For the Breinosa wellbore, which shows  $-7.8^{\circ}$  at its**  
 259 **coldest point at 78 m (and a TD at 90 m) (Juliussen et al., 2010), we extrapolated the base permafrost the local**  
 260 **geothermal gradient of  $35^{\circ}/\text{km}$  (Betlem et al., 2018; Isaksen et al., 2000). Borehole locations are shown in Fig. 1.**

261 Table 3 shows occurrences of where gas has and has not been encountered at the permafrost base. The wells in  
 262 Adventdalen, Tromsøbreen, Hopen and Gipsdalen all indicate gas accumulation at the base of permafrost and all



263 but the latter are discussed in detail here. Reindalen, Kapp Laila and the Plurdalen and Raddedalen wells on  
 264 Edgeøya are also of particular interest and discussed further because they show good evidence of permafrost, but  
 265 do not appear to encounter gas accumulations below it.

266

Well	Evidence for Gas Under Permafrost	Tentative/Shows	Permafrost but no gas
<i>Hydrocarbon Exploration</i>			
7617/7-1 Tromsøbreen-1	•		
7617/7-2 Tromsøbreen-2	•		
7625/7-1 Hopen I	•		
7625/6-1 Hopen II	•		
7714/2-1 Grønnfjorden			
7714/3-1 Bellsund			
7715/1-1 Vassdalen-2			
7715/1-2 Vassdalen-3			
7715/3-1 Ishøgda			
7721/6-1 Plurdalen			•
7722/3-1 Raddedalen			•
7811/2-1 Kvadehuken-1			
7811/2-2 Kvadehuken-2			
Kvadehuken-0			
7811/5-1 Sarstangen			
7814/12-1 Kapp Laila		•	
7815/10-1 Colesbukta			
7816/12-1 Reindalspasset			•
<i>Coal</i>			
1967-1 Adventdalen	•		
1979-10 Adventdalen	•		
1979-11 Adventdalen			•
1982-20 Adventdalen			•
Gruve 7 - H1 Adventdalen			•
DDH1B Gippsdalen	•		
1979-1 Reindalen		•	
1981 Platåberget			
1981-Breinosa			
Lunckefjellet		<i>TD above base permafrost</i>	
Ispallen			
1990-12 Slaknosa	•		
<i>Scientific Wellbores</i>			
DH1			
DH2			
DH3			
DH4	•		
DH5r	•		



DH6	
DH7a	
DH8 (Shallow)	
BH10-2008	•
Janssonhaugen	<i>TD above base permafrost</i>

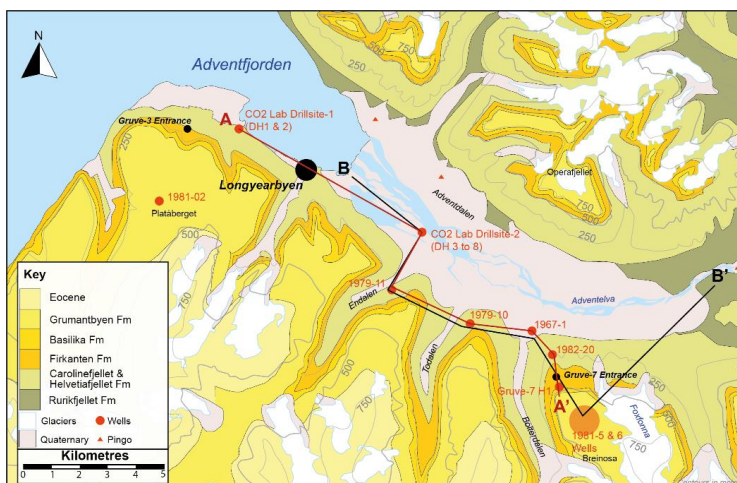
267 **Table 3** – Wells showing where gas is and is not present at the base of permafrost. Wells without a bullet either  
 268 contain no permafrost or no relevant data.

269

## 270 4.2 Case Studies: confirmed sub-permafrost gas

### 271 4.2.1 Adventdalen

272 Svalbard’s largest settlement, Longyearbyen, is located in Adventdalen (Fig. 4), and one of the better studied  
 273 areas of Svalbard (Hodson et al, 2020; Hornum et al, 2020; Johansen et al., 2003; Beka et al., 2017; Olausen et  
 274 al., 2019 and references therein). The wells of the Longyearbyen CO<sub>2</sub> Lab and coal exploration boreholes of  
 275 SNSK both show the presence of gas beneath the permafrost in Adventdalen (Fig. 5) provides a correlation panel  
 276 of these wellbores.



277

278 **Figure 4** - A Geological Map of Adventdalen showing some of the youngest stratigraphy exposed in Svalbard (base  
 279 map data courtesy of © Norwegian Polar Institute). The profile A to A’ represents the well correlation in Fig. 5 and B  
 280 to B’ the modelled permafrost profile in Fig. 6.

281 At the near-coast drillsite-1 of the Longyearbyen CO<sub>2</sub> Lab wells temperature data from DH1 and DH2 indicate a  
 282 thin permafrost interval with the base at approximately 20-30 m (Beka et al., 2017). Although sub-zero  
 283 temperatures were recorded at this site, the presence of ice is strongly dependent on the pore-fluid salinity. At  
 284 drillsite-2, wellbores DH3 and DH4 encountered overpressured water at the base permafrost. DH4 and DH5R  
 285 also encountered significant natural gas with this water kick and it was collected in gas bags for sampling (Ohm



286 et al., 2019; Huq et al., 2017). Temperature logs from well DH4 suggest base permafrost from 150 to 200 m  
287 depth but given the drilling fluid losses and mud circulation there is considerable uncertainty in this data. Cores  
288 from nearby wells DH6 and DH7A also show elevated methane levels at this depth. The water and gas influxes  
289 occur somewhere towards the middle (i.e. not top of the reservoir) of the sandstone dominated Helvetiafjellet  
290 Formation. Figure 6 is the modelled permafrost thickness in Adventdalen which shows good agreement with the  
291 independent well data observations.

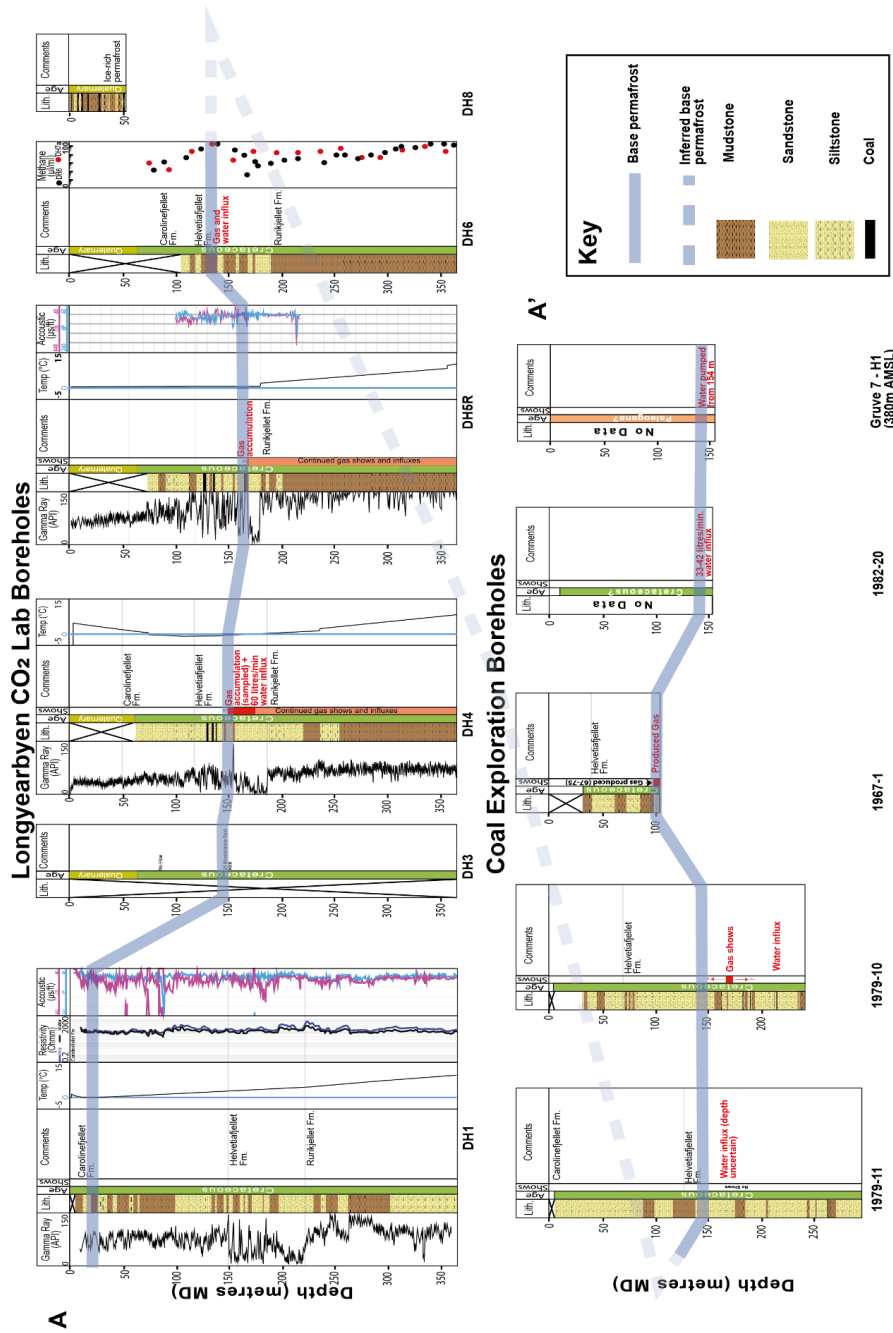


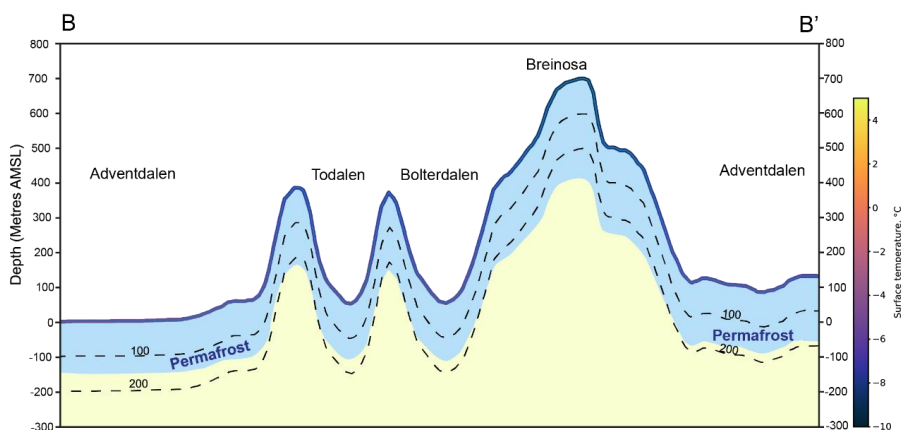
Figure 5 – A Well correlation with all available geological, drilling and petrophysical data. The location of the correlation is shown in Fig. 4. The wells in this section highlight the somewhat sporadic nature of data availability over the shallow, permafrost bearing intervals.

292

293 In the same area, hundreds of coal boreholes, drilled by SNSK over the decades, have penetrated the permafrost  
 294 interval, although data for these is more fragmented. Well 1979-11 was drilled approximately two kilometres  
 295 south of Longyearbyen CO<sub>2</sub> Lab drillsite-2 in Endalen. This well encountered water influxes with no mention of  
 296 gas, although no depths are stated in the report (Snsk, 1980, 1981). Well 1979-10, two kilometres to the



297 southeast in the neighbouring valley Todalen encountered methane-rich gas overlying inflowing water at the  
298 base of permafrost at a depth between 150 to 200 m (Snsk, 1981, 1982b; Leythaeuser et al., 1984). Well 1967-1,  
299 approximately three kilometres east and geologically updip of 1979-10, reached a depth of 106 m where a gas  
300 accumulation was encountered (Snsk, 1981). This well was also the subject of considerable interest by SNSK  
301 who investigated the potential of producing the gas commercially. Well 1982-20, approximately one kilometre  
302 southeast of 1967-1, at the base of Breinosa and the coal mine Gruve-7, did not encounter gas and took water  
303 influxes of 33-42 litres per minute at approximately 150 m at the base of permafrost (Snsk, 1982a). Another  
304 reported well, named only “first water well”, (Snsk, 1982a) in the same area flowed from the same interval at 40-  
305 50 litres per minute. Water from these two wells had a measured chloride concentration of 1500 ppm (Snsk,  
306 1982a). A well drilled inside Gruve-7 at approximately 380 m AMSL encountered liquid water at 154 m depth.



307

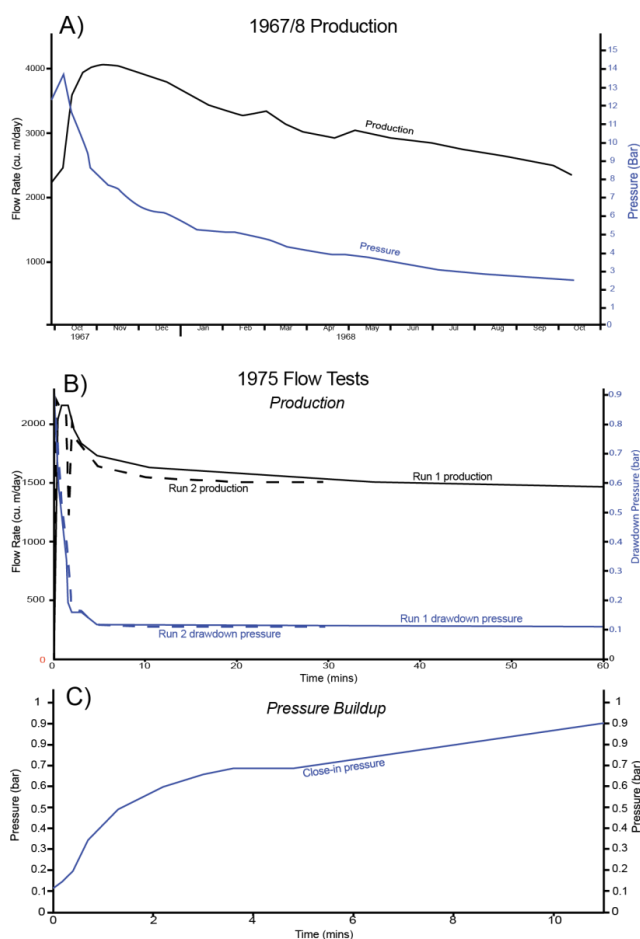
308 **Figure 6 - Modelled permafrost thickness through Adventdalen with the profile shown in Fig. 4. The model**  
309 **parameters are discussed in the methods section but note that the permafrost interval is entirely based on temperature**  
310 **rather than ice thickness or presence.**

311 Well 1967-1 and 1979-10 most likely encountered the same gas accumulation, while well 1982-20 encountered  
312 permafrost over the same stratigraphic interval and well 1979-11 is probably down-dip of the gas-water  
313 interface. Intermittent flow from the 1967-1 well was monitored between October 1967 and July 1975 (Snsk,  
314 1981). The first year of this production was continuous and monitored as shown in Fig. 7A. An initial wellhead  
315 gas pressure of 14 bar was recorded (Snsk, 1981) with relatively slow pressure and production decline over time.  
316 This indicates the gas accumulation is in the order of millions of cubic-metres and has well connected pressure  
317 support. If the aquifer pressure is known then the length of the methane gas column can be calculated from this  
318 pressure. It is clear the aquifer is not at hydrostatic pressure from the surface due to the repeated influxes and  
319 water flow from wells 1979-10, 1979-11 and in the CO<sub>2</sub> lab research boreholes. Unfortunately these pressures  
320 were not measured.

321 SNSK commissioned flow analysis work to be carried out on the 1967-1 well in July 1975 and the results of  
322 these two test runs are shown in Fig. 7B. Here it is clear the well responded to pressure drawdown. However,  
323 flow rates were still significantly lower than those recorded over the first year. Figure 7C shows the pressure



324 build-up when the well was shut in (effectively closed from the atmosphere) between the two test runs. The  
325 quick return to pre-drawdown pressures indicates **sp** what unsurprisingly, a good natural pressure support in  
326 the well. Ultimately the gas here was deemed by Statoil, and consequently SNSK, to be an uneconomic  
327 accumulation locally trapped by permafrost (Snsk, 1981).



328

329 **Figure 7 – Production tests on the 1967-1 well in Adventdalen where was produced and flared. A) Gas production and**  
330 **pressure depletion for the first year of production. B) An oilfield-standard production test of production and pressure**  
331 **drawdown carried out by Statoil in 1975. The relatively fast flattening of the curves suggests stable flow and strong**  
332 **pressure communication in the reservoir. C) Pressure build up following shut-in of the well also indicating**  
333 **appreciable fluid communication.**

334 A drilling summary (Snsk, 1982a) documents two wells drilled at approximately 400 m above mean sea level  
335 (AMSL) on Platåberget, on the southern side of Adventdalen. They both report total drilling fluid losses at 160 -  
336 170 m MD with no record of gas influxes. This is within the permafrost interval based on the presence of  
337 permafrost in the coal mine, Gruve-3, some 200 m below the surface. This demonstrates that the permafrost  
338 interval here is permeable. Similarly, on Breinosa, where the Gruve-7 mine is situated some fifteen kilometres to



339 the east, wells 81-05 and 81-06 both encountered total fluid losses at a similar depth of 170m (Snsk, 1982a), well  
340 within the permafrost interval (Juliussen et al., 2010). The mine itself is situated entirely within the permafrost  
341 interval and has suffered from meltwater influxes from the overlying cold-based glacier, Foxfonna, on numerous  
342 occasions (Christiansen et al., 2005). Similar losses occurred in several intervals between 106 and 196 m in well  
343 19-2011 on Operafjellet, a plateau on the northern side of Adventdalen (Snsk, 2011a). Freezing in the wellbore at  
344 132 m indicates at least some, if not all, of these losses occurred in the permafrost interval.

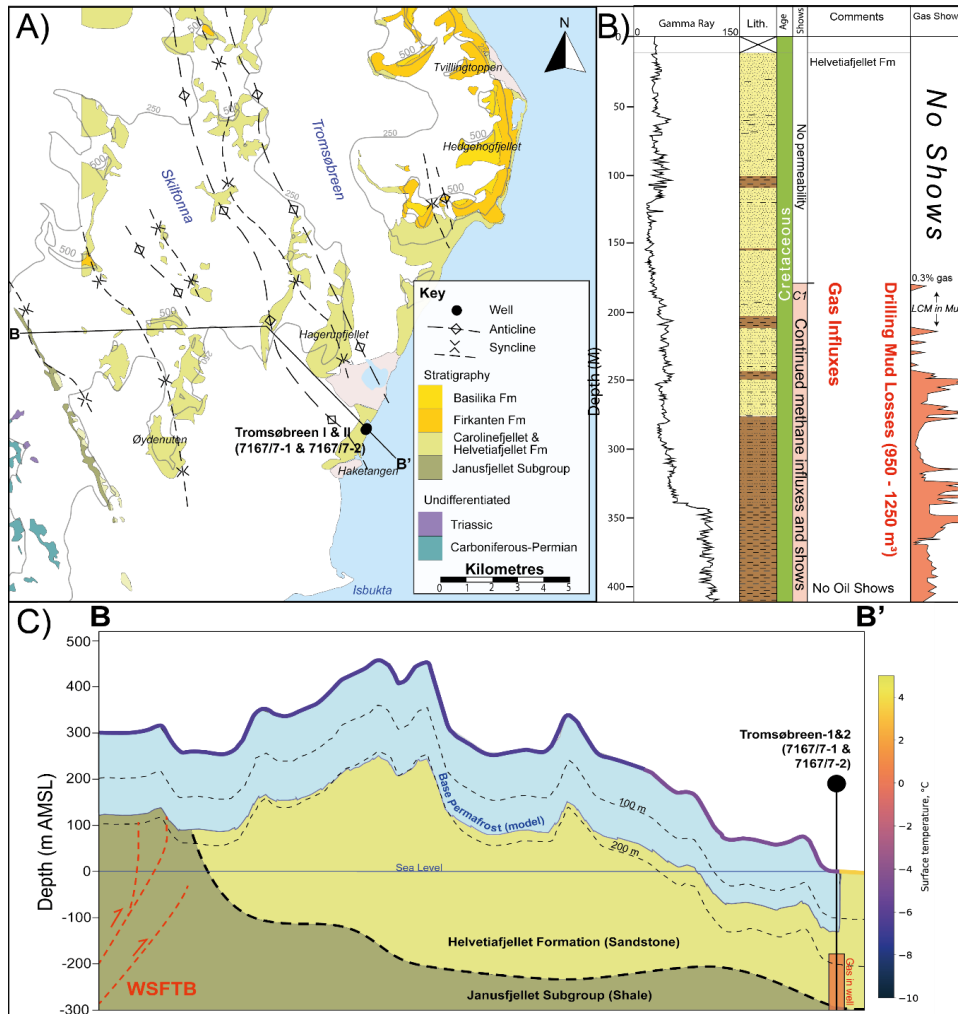
345 Five pingos are situated along the northern edge of Adventdalen. Four of them provide active migration  
346 pathways through the permafrost leading to the discharge of brackish springs and high concentrations of methane  
347 (up to and marginally exceeding the solubility limit of 41 mg L<sup>-1</sup>) (Hodson et al., 2020). At the easternmost  
348 pingos, the chloride concentrations and the <sup>13</sup>C isotopic composition of both the methane and dissolved CO<sub>2</sub> are  
349 remarkably similar to those described in the wellbore records above.

#### 350 **4.2.2 Tromsøbreen**

351 Two hydrocarbon exploration wells, Tromsøbreen-I (7617/1-1) and Tromsøbreen -2 (7617/1-2), were drilled at  
352 Haketangen in south-eastern Spitsbergen in 1977 and 1988, respectively. Both were drilled in nearly the same  
353 coastal location at 6 m AMSL, near the terminus of the Tromsøbreen glacier (Senger et al., 2019).

354 The wells primarily targeted the Jurassic-Triassic sandstones in an anticline trap mapped on the surface to the  
355 west (Fig. 8A) with the wells planned to be slightly deviated to intersect this at the prospect depth (Norsk Polar  
356 Navigasjon a/S, 1977b, a; Polargas Prospektering Kb, 1988). The outcrops in this area are predominantly the  
357 Carolinefjellet and Helvetiafjellet sandstones, though older stratigraphy outcrops to the west near the WSFTB  
358 hinterland. Unfortunately, gamma ray was the only petrophysical data acquired over the shallow intervals,  
359 though gas chromatography, drilling parameters and drilling and well reports provide a good indication of the  
360 subsurface.

361 Both wells suffered major drilling problems at the apparent base of permafrost at 179 m. The permafrost interval  
362 showed no permeability and in Tromsøbreen-1 took 45 days (the entire wellbore took 90 days) to successfully  
363 drill through (Norsk Polar Navigasjon a/S, 1977b). Both wells suffered major drilling fluid losses into the  
364 formation; this was measured in Tromsøbreen-1 at 150 to 200 barrels (24 to 32 cubic metres) of drilling mud  
365 (Norsk Polar Navigasjon a/S, 1977b). At the same time as drilling fluid was lost from the wellbores, gas influxes  
366 into the both wells also occurred. Indeed, measurements show significant natural gas from this point  
367 continuously until the Triassic stratigraphy including a gas kick at 960 m in Tromsøbreen-1. Immediately after  
368 the first gas influx lost circulation material was used to remedy drilling fluid losses. Lost circulation material is  
369 used to plug cavities in the formation to prevent further losses, it also renders the mud gas traps unusable over  
370 the interval it is used, as is shown by “LCM in mud” in Fig. 8B. The shallowest gas sample was taken at 768 m  
371 and comprised predominantly methane and is discussed later in this section. Gas observed throughout the  
372 intervals of both wellbores was deemed by the operator as important enough to plan a third well approximately  
373 one kilometre to the north (Polargas Prospektering Kb, 1988), although it was never drilled.



374

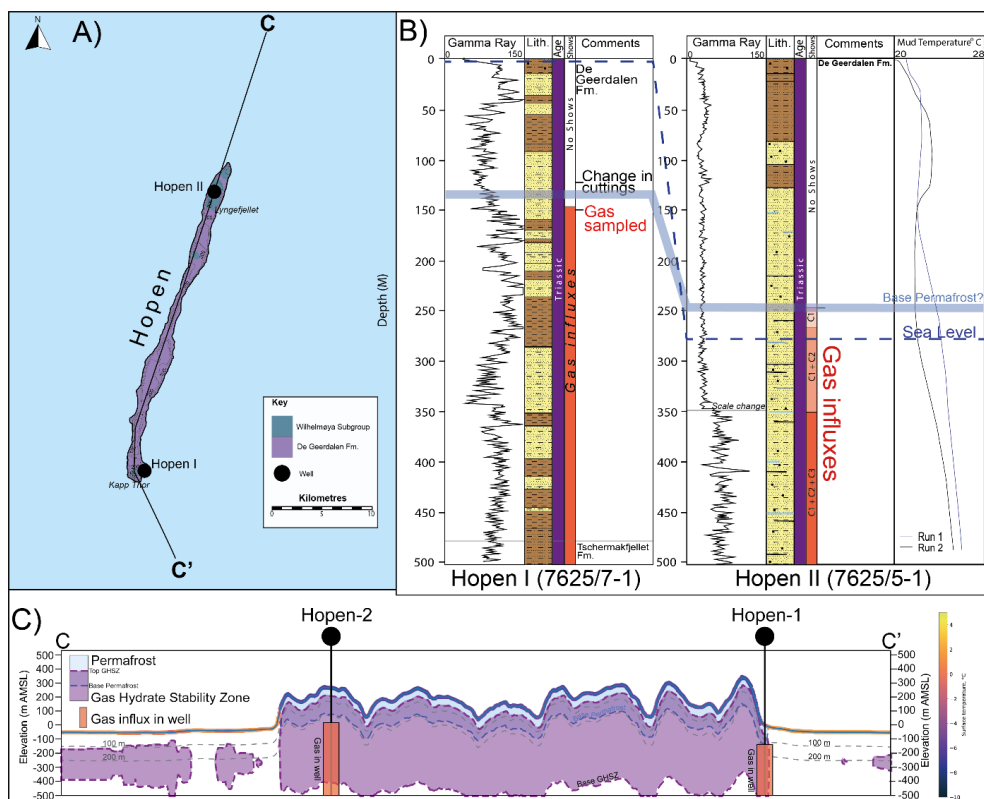
375 **Figure 8** – A) Geological map from Tromsøbreen redrawn from Birkenmajer et al. (1992). B) All available data over  
 376 the shallow intervals at Tromsøbreen combined from the two wells. The petrophysical, lithological and gas data is  
 377 from 7617/7-1 (Tromsøbreen I) while 7617/7-2 (Tromsøbreen II) recorded very little data over the shallow intervals,  
 378 though did corroborate drilling fluid losses and gas influxes at the same depths. C) Cross-section (shown in A) of  
 379 modelled permafrost thickness and the important reservoir and sealing formations, and inferred faults of the West  
 380 Spitsbergen Fold and Thrust Belt (WSFTB) based on outcrop data (Birkenmajer et al, 1992).

381 Based on bottom-hole temperatures in both wells, the Tromsøbreen area has an extremely high geothermal  
 382 gradient, with averages for Tromsøbreen-2 suggesting 43°C/km and Tromsøbreen-1 indicating 52°C/km (Betlem  
 383 et al., 2018). Fig. 8C shows a simple modelled permafrost thickness using this geothermal regime and surface  
 384 temperatures. The apparent permafrost encountered in the wellbores has a discrepancy with the steady-state  
 385 assumption model of approximately forty metres.



#### 386 4.2.3 Hopen

387 The island of Hopen is 34 km long and 0.5-2.5 km wide and is comprised almost entirely of the heterolithic  
388 Triassic De Geerdalen Formation, which is approximately 650 m thick here (Lord et al., 2014). Two wells were  
389 completed on Hopen, Hopen-1 (7625/7-1) and Hopen-2 (7625/5-1), drilled in 1971 and 1973, respectively  
390 (Senger et al., 2019). Hopen is one of the few cases where the operator took interest in the sub-permafrost gas  
391 accumulation and sampled it. Hopen-1 was drilled on the southern beach while Hopen-2 was drilled in the  
392 highlands in the northern part of the island (Fig. 9).



393

394 **Figure 9 – A) Geology and outline of the island of Hopen based on Lord et al. (2014) with the map location shown in**  
395 **Fig. 1). Profile C-C’ is shown in C) B) Petrophysical and lithological information from the respective wells. Gas**  
396 **samples were taken in Hopen I while a chromatograph in the mud traps was used in Hopen II. The muted gamma ray**  
397 **response in the upper 350 m of Hopen II is probably due to the recording through casing. C) Cross sectional (shown in**  
398 **A) of Hopen showing the modelled permafrost and gas hydrate stability zones. Geology is not shown but the section**  
399 **comprises almost entirely of the heterolithic sand, siltstone and shales of the De Geerdalen Formation.**

400 Both wells sustained gas influxes attributed to the base of permafrost (Norske Fina a/S, 1971a, b, 1973b, a). In  
401 terms of petrophysical data, operations at Hopen-1 only acquired gamma ray data over the uppermost interval  
402 while Hopen-2 gathered gamma ray and temperature data. However, it is important to note that the wells also  
403 used heated drilling fluids to prevent freezing in the permafrost interval so absolute temperature values in this



404 section are of limited use. Gas samples were taken in the Hopen-1 well from approximately 150 m while at  
405 Hopen-2 a gas chromatograph was used in the drilling mud traps. Based on temperature data from these wells the  
406 geothermal gradient of Hopen is 25-34°C/km (Betlem et al., 2018).

407 Hopen-1 was drilled on the southern coast and encountered a gas kick at approximately 150 m which was  
408 deemed significant enough to be sampled. This gas is much heavier in composition than the gas encountered in  
409 Adventdalen and Tromsøbreen and is discussed later in this section. The wellsite geologist noticed an abrupt  
410 change in the cuttings characteristics, but not their lithological composition, at 138 m (Norske Fina a/S, 1971b)  
411 which was attributed to the base of permafrost. Gas was recorded from permafrost base to the bottom of the well  
412 at 908 m (Norske Fina a/S, 1971a, b).

413 Hopen-2 was drilled approximately 30 km further north on Lyngefjellet. Elevated gas readings in returning  
414 drilling mud were recorded from approximately 250 m (approximately 30 m AMSL) with no apparent changes in  
415 cutting lithology.

#### 416 4.2.4 Slaknosa and Kapp Amsterdam

417 In 1990 SNSK's 399 m deep coal exploration wellbore 1990-12 encountered a gas blowout at around  
418 approximately 550 m AMSL on Slaknosa plateau on the southern edge of Reisdalen (Snsk, 1991). The blowout  
419 exerted enough force to blow rocks, gravel and gas out of the wellbore. Little data remains from this wellbore  
420 and the exact interval of the gas kick is unknown although it was hypothesised to originate from fractured  
421 intervals having migrated from nearby coal seams.

422 Kapp Amsterdam is a cape close to the mining settlement of Svea. It is comprised of a glacial moraine  
423 approximately 600 years old (Kristensen et al., 2009). In 1986 a methane blowout occurred when drilling  
424 through these deposits at a depth of 33.5 m (Snsk, 1986). According to the drilling report, thermistors were  
425 placed in the wellbore with suggestion that permafrost was acting as a top seal (Snsk, 1986).

#### 426 4.2.5 Gipsdalen

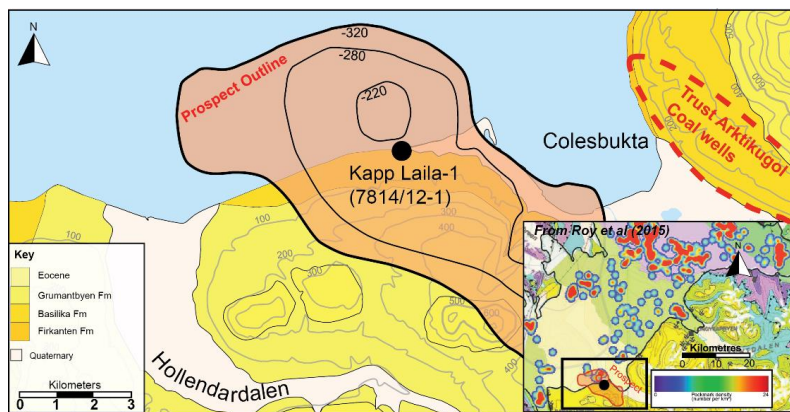
427 There are very limited data from Gipsdalen, but a single drilling summary report (Senger et al., 2019; Snsk,  
428 1982b, 1979) shows that eight coal exploration wells were drilled in the area. One of these, DDH7, encountered  
429 overpressured water at the base of permafrost at 200 m in either Permian or Carboniferous rocks. The basis for  
430 determining base permafrost is not given but the report states a depth of 300 m was expected prior to drilling.  
431 Another well, DDH1, suffered a gas kick from the same apparent interval. The wellhead pressure from the water  
432 influx in DDH7 was 23 bar while no flow rates were recorded. If the aquifer overpressure is artesian, it equates  
433 to a hydraulic head at approximately 330 m AMSL which may correlate to recharge from heavily glaciated areas  
434 to the east.

435



436 **4.3 Case studies: Permafrost present with no trapped gas**

437 **4.3.1 Kapp Laila and Colesbukta**

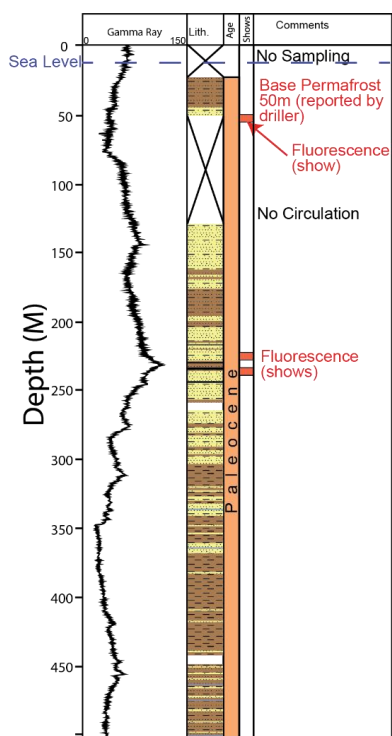


438

439 **Figure 10 - Map of the Kapp Laila area (based on SNSK, 1994 and data courtesy of © Norwegian Polar Institute) with**  
440 **the SNSK prospect and well location shown. Inset is a map of pockmarks on the seafloor of Isfjorden from Roy et al**  
441 **(2015). A high concentration of pockmarks on the seabed apparently overlies the crest of the prospect. The map**  
442 **location is shown in Fig. 1.**

443 Given the coastal location, permafrost is considered to be relatively thin, if present, and is almost certainly absent  
444 further offshore (Majewski and Zajaczkowski, 2007). Data from the Trust Arktikugol Colesbukta hydrocarbon  
445 exploration well (7815/10-1) is very limited though gas was reported to flow from deeper Triassic intervals  
446 (Senger et al., 2019). The SNSK Kapp Laila hydrocarbon exploration well (7814/12-1) does document some  
447 fifty metres of permafrost; although it is unclear on what information this is based on (Snsk, 1994). The well and  
448 prospect locations are shown in Fig. 10, interesting the crest of the prospect coincides with a cluster of  
449 pockmarks offshore (Roy et al., 2015). Gas shows in the form of dull yellow fluorescence were also documented  
450 at 44-52 m (Fig. 11), which coincides with the stated permafrost depth. It is important to note that fluorescence  
451 shows are not unequivocal proof of hydrocarbons and that yellow fluorescence can also be caused by dolomite  
452 and aragonite, although there is no evidence of these minerals in this interval. We have also identified methane  
453 seeps through a pingo system approximately 8 km to the east at Trodalen which are the subject of ongoing  
454 research in the area.

455 Trust Arktikugol coal boreholes from the early twentieth century apparently typically encountered permafrost at  
456 100 m depth (Lytkevich, 1937). Though no specific wells are mentioned, the approximate location of these  
457 boreholes is highlighted in Fig. 10. These wells also encountered artesian water at depths of 229-339 m which  
458 flowed at 110 litres per minute (Lytkevich, 1937).



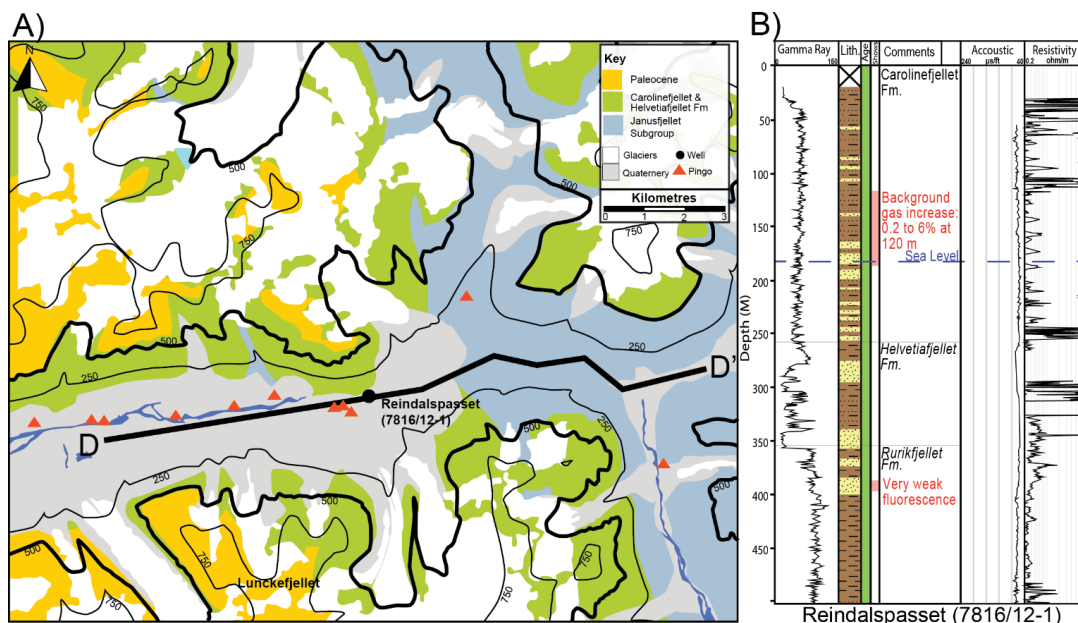
459

460 **Figure 11** Kapp Laila well with all available data and geological and drilling comments. Minor gas shows occur  
461 at 50 m depth which coincides with the stated base of permafrost (SNSK, 1994).

#### 462 4.3.2 Reindalen

463 The Reindalspasset well (7816/12-1) was drilled in 1991 by SNSK and Norsk Hydro and was the first well to  
464 target a prospect identified by seismic data (Senger et al., 2019). It also has a good set of petrophysical data over  
465 the permafrost-bearing interval. The Reindalen well is situated on the eastern fringes of the Central Tertiary  
466 Basin (Fig. 12A) but its primary target was a deeper rotated fault block of the Carboniferous Billefjorden  
467 zone. Well data suggests a geothermal gradient of 31°C/km (Betlem et al., 2018). Another observation of this  
468 area is the prevalence of pingos in the valley to the east and west which are indicative of migration pathways  
469 through the permafrost, some of which also exhibit methane seepage.

470 The well data shown in Fig. 12B demonstrates the challenges in identifying permafrost from petrophysical data,  
471 particularly in Svalbard where rocks are typically overcompacted. The rapid resistivity cycling in upper parts is  
472 likely due to thawing of permafrost and intermittent invasion of highly conductive, saline drilling fluids, though  
473 this is purely speculative. There are no major indicators in the acoustic data. Indeed, in both acoustic and  
474 resistivity data, probably due to low porosity in the permafrost bearing zone. The first good quality sandstone  
475 intervals at around 170 m do possess low resistivities which are probably indicative of liquid water. Although the  
476 2D seismic line is of good quality the permafrost does not manifest itself for reasons previously discussed.



477

478 **Figure 12 – A** A Geological map of Reindalen ( base map data courtesy of © Norwegian Polar Institute) with the  
 479 **Reindalspasset** borehole shown. Lunckefjellet plateau is also shown, where several coal boreholes that experienced  
 480 **fluid losses**. The map location is shown in Fig. 1. B) The petrophysical log over shallow intervals in Reindalspasset  
 481 (7816/12-1). The well sits in the valley of Reindalen where a series of pingos are situated updip from the wellbore, on  
 482 the north side of the valley. Line D to D' shows the location of the seismic line shown in Fig. 17.

483 No accumulations or gas influxes occurred in upper parts of this well though a background gas increase was  
 484 observed. A 12 ¼" (31.115 cm) pilot hole was drilled to 164 m and background gas was recorded steadily at  
 485 0.2%. This hole was subsequently opened up to the planned 16" (40.64 cm); at 120 m depth background gas  
 486 suddenly rose to 6% (Norsk Hydro, 1991). Because widening the hole resulted in greater fluid circulation,  
 487 drillers and the wellsite geologist attributed the rise in gas due to thawing of the permafrost. They further  
 488 speculated that it may be due to hydrate dissociation, though as no samples or pressures were measured this  
 489 hypothesis remains impossible to assess. It is also important to note that this occurred in a low permeability  
 490 siltstone interval where any gas accumulations are unlikely to flow at a good rate.

491 At Lunckefjellet, approximately 5 km southwest of the 7816/12-1 hydrocarbon well, permafrost has been  
 492 demonstrated to be approximately 5 m thick (Juliusen et al., 2010). Drilling fluid losses were encountered in  
 493 several boreholes on the plateau (Snsk, 2011b, c, d), well within the permafrost interval.

494

### 495 4.3.3 Edgeøya

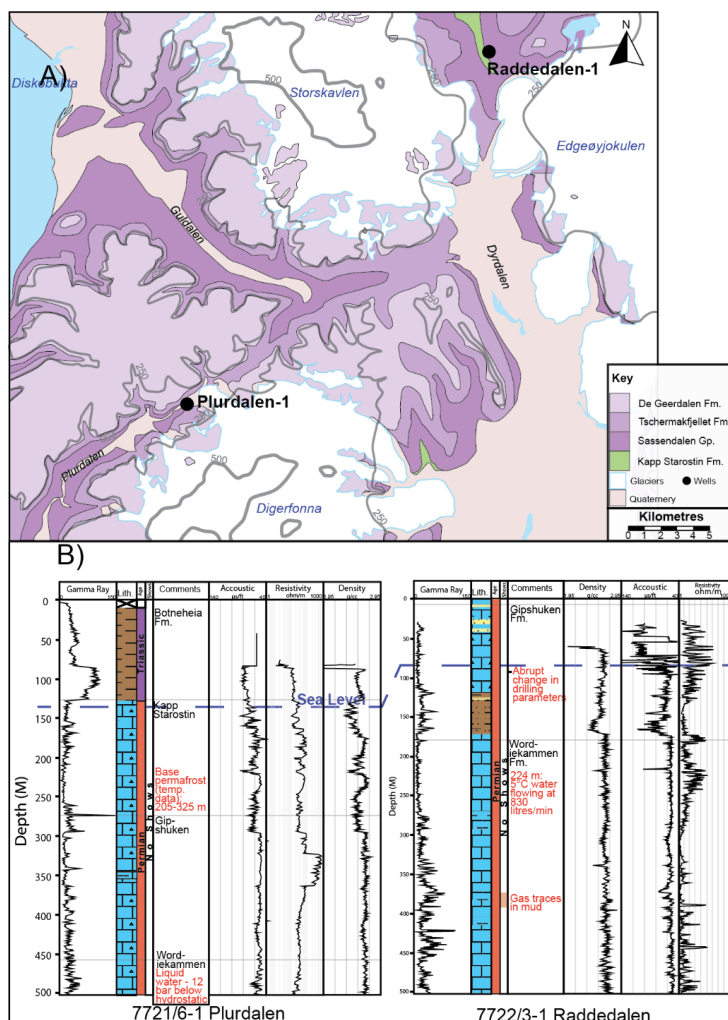
496 The Plurdalen (7721/6-1) and Raddedalen (7722/3-1) wells are some 29 km apart (Fig. 13A) and were both  
 497 drilled in 1972 by different operators. They both penetrate thick Permian carbonates and Carboniferous rift



498 successions. The uppermost 130 m of the Plurdalen well also encounters the lowermost parts of the Triassic  
499 Botneheia shales.

500

501 The permafrost base here occurs in very hard, low porosity and low permeability rocks. Because of this  
502 petrophysical data are, again, somewhat ambiguous here. Indeed, at Raddedalen the hard rocks in combination  
503 with permafrost meant the well initially failed to make any progress during spudding (Total Marine Norsk,  
504 1972). Drilling the upper hundred metres was very slow and wellbore cavings were also common, possibly due  
505 to permafrost thawing. The drilling report for Raddedalen suggested the permafrost base was at 95 m (Total  
506 Marine Norsk, 1972). They based this on resistivity peaks above 5000  $\Omega$ m at depths shallower than 95 m, but not  
507 deeper, though we also note that this resistivity drop also coincided with a lithological change to shale. The  
508 report also describes cycling and skipping in the acoustic log over this depth due to intermittent tool contact with  
509 the wellbore wall caused by thawing at the permafrost base. The Raddedalen well data in Fig. 13B shows this but  
510 also demonstrates that this skipping begins nearer 60 m depth. A water influx occurred at 224 m and probably  
511 originated from the carbonate Wordiekammen Formation. The water influx was measured at 830 litres a minute  
512 and had a temperature of 5°C, so clearly is from well below permafrost. Assuming the well-derived geothermal  
513 gradient of 30°C/km (Betlem et al., 2018) this would put the base permafrost at 57 m depth, which matches well  
514 with the observed skipping in the acoustic log. The aquifer is also overpressured by 4.41 bar and probably of  
515 artesian origin.



516

517 **Figure 13 - A) Geological map of central western Edgeøya (base map data courtesy of © Norwegian Polar Institute)**  
 518 **showing the two hydrocarbon exploration wells on the island. The map location is shown in Fig. 1. B) Petrophysical**  
 519 **logs from the hydrocarbon exploration wells at Plurdalen (7721/6-1) and Raddedalen (7722/3-1).**

520 At Plurdalen, a more complete set of petrophysical logs shows no clear evidence of permafrost or base  
 521 permafrost. Temperature data apparently (Norske Fina a/S, 1972b, a) suggests base permafrost anywhere from  
 522 205 to 325 m. The log data does not appear to show any similar characteristics used to determine the base  
 523 permafrost of the Raddedalen well. Liquid water, probably in the same Wordiekammer interval as at the  
 524 Raddedalen well, was encountered at approximately 500 m. The temperature or salinity of this water was not  
 525 recorded but, surprisingly, the pressure was 12 bar below hydrostatic. The most likely explanation for the  
 526 underpressure is due to outflow and equilibrium with the fjord to the west, as 12 bar of underpressure at the  
 527 wellhead corresponds to a hydraulic head approximately at sea level.



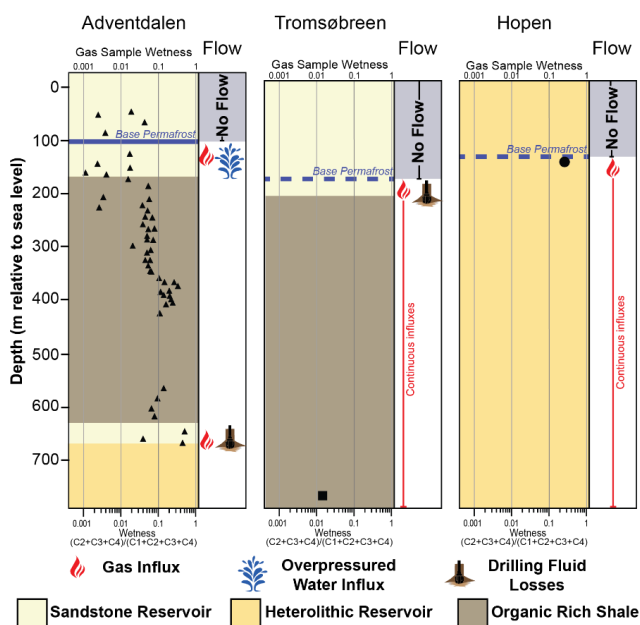
528 Neither wells encountered hydrocarbons, neither did the Plurdalen well report any shows. Raddedalen had minor  
529 gas shows between 387-390 m and a trace increase in background gas in the mud returns (Norske Fina a/S,  
530 1972a; Total Marine Norsk, 1972).

#### 531 4.3.4 Petuniabukta

532 At Petuniabukta, Verba (2013) describes gas accumulations in Carboniferous reservoirs that do not have an  
533 overlying lithological seal due to denudation and inclined and outcropping bedding. The author suggests a  
534 permafrost interval of 250 to 400 m where no liquid water was encountered and suggests this must be sealing.  
535 Oil has also been encountered in the area in small quantities (Senger et al., 2019). This indicates the  
536 accumulations are likely thermogenic and that there are source rocks capable of generating and expelling  
537 hydrocarbons, at least locally.

538

#### 539 4.4 Gas Samples – Adventdalen, Tromsøbreen and Hopen



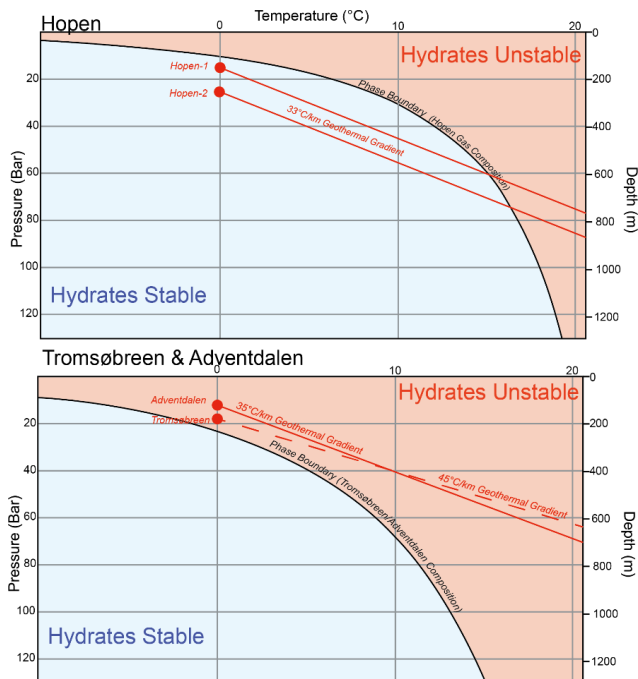
540

541 **Figure 14 – Gas wetness from samples taken in wells from Adventdalen (Ohm et al, 2019), Tromsøbreen (Norsk Polar**  
542 **Navigasjon A/S, 1977b) and Hopen (Norske Fina A/S, 1972). The Hopen gas is much heavier and thus more prone to**  
543 **form hydrates at lower pressures and higher temperatures than methane.**

544 Gas samples were taken by hydrocarbon exploration wells at Tromsøbreen and Hopen, with three samples taken  
545 at each. Their compositions are shown in Table 4. A comprehensive analysis of the gas at the Longyearbyen CO<sub>2</sub>  
546 was carried out by Ohm et al. (2019) and Huq et al. (2017), and a rudimentary analysis of the coal borehole gas  
547 discovery was carried out by Snsk (1981). These analyses of the gas accumulation and analysis of seeps of the



548 pingo systems in the area (Hodson et al., 2019) show the base-permafrost accumulation is methane dominated.  
549 The more extensive analysis of the Longyearbyen CO<sub>2</sub> Lab gas provides a more complex story throughout the  
550 entire stratigraphy with contributions from biogenic and thermogenic sources (Ohm et al., 2019). The sub-  
551 permafrost gas at Hopen is much wetter and clearly from a thermogenic origin. Analysis at Tromsøbreen was  
552 taken from gas much deeper than that encountered at base permafrost. However, it shows this gas is relatively  
553 dry although still likely to be thermogenic due to the sample depth of 768 m and its extraction directly from the  
554 Agardhfjellet Formation source rock (Norsk Polar Navigasjon a/S, 1977b, a). Figure 14 shows the wetness of gas  
555 from the three locations, wetter gas means it has a greater component of heavier hydrocarbon molecules such as  
556 ethane or propane.



557

558 **Figure 15** – The upper graph shows the natural gas hydrate stability diagrams for the Hopen gas composition (Table  
559 4). The lower graph shows the same for the Adventdalen (well DH4) and Tromsøbreen methane dominated gas  
560 compositions (Table 4 and Fig. 14). Red circles represent the base permafrost (0° C) depths using pressures based on a  
561 hydrostatic gradient from the surface. Lines represent stability with increasing depths at each locality based on local  
562 geothermal gradients (Betlem et al., 2018; Isaksen et al., 2000).

563 The composition of the gas is important in understanding its potential phase in the subsurface. Figure 15 shows  
564 phase diagrams for the gas compositions and thermobaric conditions at Hopen, and at Adventdalen and  
565 Tromsøbreen. While the dry gas at Tromsøbreen and Adventdalen is unlikely to be in hydrate form at their points  
566 of discovery, the gas at Hopen is much wetter. As a consequence, it is more susceptible to be thermodynamically  
567 stable as gas hydrate form (Betlem et al., 2019). In light of this, we modelled the potential gas hydrate stability



568 zone over Hopen based on the sampled composition. Figure 9C shows a thick zone where natural gas hydrates of  
 569 this composition are likely stable.

Sample Number	Sample run 1	Sample run 2	Sample run 3	Sample run 1	Sample run 2	Sample run 3
<b>Hydrocarbons</b>	<b>7617/7-1 (Tromsøbreen I)</b>			<b>7625/7-1 (Hopen I)</b>		
<b>C1</b>	64.79 - 70.81	68.57	63.84	92.35	94.97	97.24
<b>C2</b>	20.23 - 18.67	18.20	20.21	0.11	0.05	0.49
<b>C3</b>	10.97 - 7.76	9.26	11.10	0.09	0.01	0.16
<b>C4</b>	3.51 - 2.46	3.39	4.08	0.18	0.06	0.20
<b>C5+</b>	0.58 - 1.32	1.22	0.79	0.97	1.03	0.96
<b>Nitrogen</b>	Abnormally High (not quantified)			6.26	3.86	0.91
<b>CO2</b>	-			0.04	0.02	0.04
<b>Gravity</b>	-			0.609	0.600	0.591

570 **Table 4 – Geochemical data from samples taken at the hydrocarbon exploration wells at Tromsøbreen-1 and Hopen-1.**

571

## 572 5 Discussion

### 573 5.1 Identifying base permafrost

574 The active layer and upper parts of the permafrost interval are well-studied in Svalbard (Westermann et al., 2010;  
 575 Rachlewicz and Szczuciński, 2008; Strand et al., in press). However, the base permafrost is rarely the focus of  
 576 study with data coming overwhelmingly from industrial boreholes. Petrophysical data from predominantly  
 577 hydrocarbon wells may show some fluid trends that can be attributed to the transition from ice-bearing to water-  
 578 bearing strata. However, the complex geology largely overprints fluid responses. This is most likely due to the  
 579 generally low porosity of the rocks due to overcompaction due to deep burial and subsequent uplift.

580 Additionally, it may be reflective of the diffuse nature of the base permafrost. The most robust cases  
 581 demonstrating the base permafrost actually occur where there is very little change in the petrophysical data.  
 582 Because geology, rather than fluid content dominates the petrophysical response, the clearest cases are where  
 583 there are sudden fluid influxes into the wellbore with no change in the geological properties of the reservoir rock  
 584 itself. These influxes with no apparent lithological top seal occur in numerous locations throughout Svalbard,  
 585 most notably in multiple wells in Adventdalen, Hopen, Tromsøbreen, Gipsdalen, and Petuniabukta. These  
 586 occurrences show no particular prevalence with respect to age or depositional setting of the reservoir.

587 Permafrost is typically not considered to be present in coastal areas of Svalbard. However, evidence from  
 588 Tromsøbreen, and possibly also at Hopen, Petuniabukta and Kapp Laila, suggest that ice-bearing permafrost is  
 589 present in these areas (Fig. 3) and may even continue offshore.

590 The area  re permafrost has been modelled shows broad agreement with well-based observations in the  
 591 areas. Discrepancies are due to both the fact the modelled permafrost is based on temperatures, as per definition,  
 592 while well-based observations identify the base of ice-bearing permafrost which is also dependent on water  
 593 content, flow and its salinity. In addition, subsurface complexities are not captured in the model, for example the  
 594 forty-metre discrepancy between modelled and observed permafrost at Tromsøbreen is probably additionally

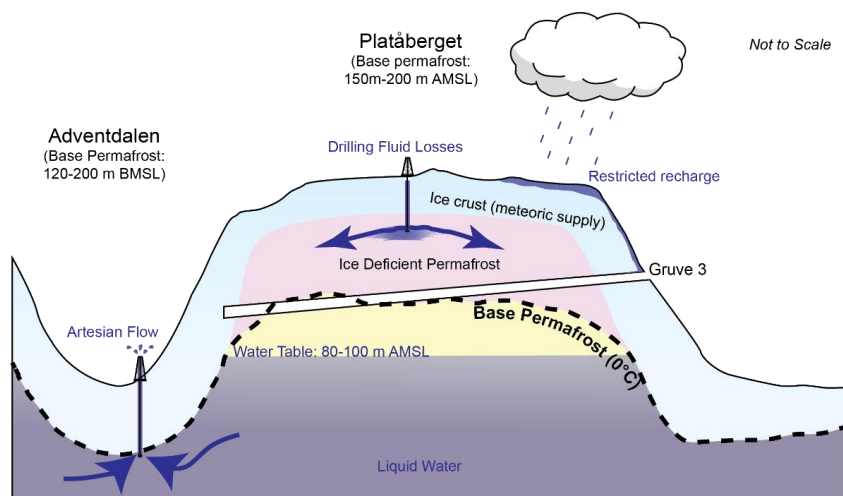


595 influenced by an overestimation of the geothermal gradient, the complex local geology and is in a heavily  
596 glaciated area.

597

## 598 5.2 Permafrost formation and sealing effectiveness

599 Theoretically, the permafrost interval should form an extremely effective seal or “cryogenic cap”. If ice-bound it  
600 is impermeable, often thick and has the ability to self-seal through freezing water in the event of fracturing. In  
601 reality the story is a little more complex and the seal-forming process is extremely poorly understood. An  
602 effective permafrost seal is demonstrable in various locations in Svalbard by the presence of gas and abnormally  
603 pressured water at the base of permafrost. This appears to be the case where the permafrost zone is ice-saturated,  
604 most notably in valley settings. The previously described drilling losses in wells on the plateaus of Platåberget,  
605 Breinosa Operafjellet, Lunckefjellet in addition to Ispallen (Snsk, 2014, 2013a, b, c) occurred in known  
606 permafrost intervals (Juliussen et al., 2010). This suggests that in these highland areas, at least, that permafrost is  
607 not forming a continuous impermeable seal.



608

609 **Figure 16 – Schematic cross section of the permafrost interval at Platåberget. Artesian pressures in the valley wellbore**  
610 **1967-1 suggest an elevated water table (Table 5) which still sits below the base of permafrost in the mountain. The**  
611 **lack of water supply from below during permafrost formation leads to a dry and permeable permafrost interval and**  
612 **subsequent drilling losses. Similar drilling fluid losses appear common in the permafrost interval in several plateau**  
613 **areas in Svalbard. In the valleys the permafrost interval forms through the water table and results in a thick**  
614 **impermeable ice seal.**

615 The valley-based permafrost interval has been shown to contain a proportion of liquid water (Keating et al.,  
616 2018) in the form of microfilms and hypersaline pockets. Despite this, the interval remains impermeable to both  
617 water and gas. Gas accumulations beneath the permafrost appear to be common and widespread regardless of  
618 stratigraphy (Figs. 2, 3 and Table 3) which demonstrates the good sealing potential. Abnormal pressures are  
619 common at the base of permafrost in several locations in Svalbard which demonstrates the sealing properties of  
620 the overlying permafrost. The best data is in Adventdalen where sudden, slightly saline, water influxes occur at



621 the base of permafrost in the Helvetiafjellet Formation. The strong and sustained flow rates indicate appreciable  
622 lateral connectivity within the aquifer, indicating an artesian origin of overpressure. The current view of this  
623 overpressure is attributed to the formation of permafrost (Hornum et al., 2020) but the high flow rates  
624 (Magnabosco et al., 2014), reservoir connectivity and its outcropping beneath the fjord to the west (Björnsdóttir et  
625 al., 2012) discount this.

Case	High	Low
<b>Contact</b>	160 m	210 m
<b>Buoyancy Pressure (gas SG = 0.5537)</b>	7.1 bar	9.3 bar
<b>Aquifer Overpressure</b>	6.9 bar	4.7 bar
<b>Hydraulic Head Elevation (well: 32.5 m)</b>	103 m AMSL	79.2 m AMSL

626 **Table 5 – Aquifer pressure calculation from wellhead pressures in well 1967-1 and the possible gas-water contact**  
627 **wellbore 1971-10. The low case uses a saline water pressure gradient of 0.10067 bar/m while high case uses freshwater**  
628 **gradient of 0.09795 bar/m.**

629

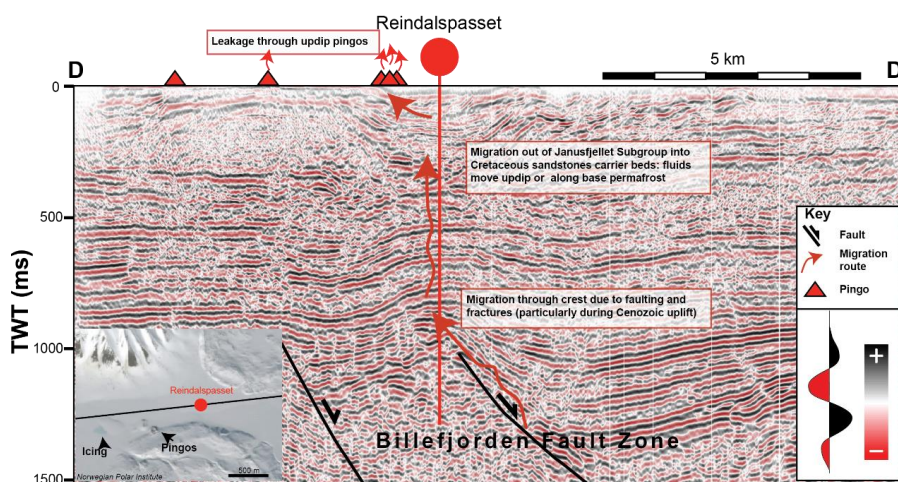
630 In highland areas the role of permafrost as a seal is less clear. Gas blowouts, like the documented occurrence in  
631 well 1990-12 on Slaknosa plateau, were quite common based on anecdotal evidence. In the case of Slaknosa it is  
632 likely that the permafrost acts as a seal. This is because the formations outcrop in the cliff sides so must require a  
633 seal strong enough to withhold significant buoyancy pressure both above and laterally in the reservoir. However,  
634 in other highland areas, including on Platåberget and Breinosa on the southern side of Adventdalen, the  
635 permafrost interval appears to not be fully ice saturated.

636 The difference between the permafrost sealing potential in highlands and valleys can be explained by the  
637 availability of water and the permafrost formation mechanism. Permafrost forms from the top-down, and as it  
638 forms near the surface, it restricts the amount of meteoric input from the surface. As the permafrost thickens, a  
639 water deficiency will develop if the water table remains deeper than the base of permafrost. Present day  
640 pressures in Adventdalen (Table 5) suggest a hydraulic head well below the base permafrost which may explain  
641 the water deficiency within the permafrost interval. This may lead to a thinner permafrost seal with potential  
642 migration pathways through it, which may explain perennial springs at elevations up to 350 m around Breinosa.  
643 In valley settings, the permafrost develops below the water table so there is always plentiful access to water,  
644 resulting in a thick ice-saturated interval. This difference in water-availability during permafrost formation may  
645 be critical to the development of an effective permafrost seal and explains why highland wells, such as those on  
646 Platåberget, suffer drilling losses whilst those in the valley do not (Fig. 16). At Slaknosa, which is a highland  
647 setting, the permafrost likely developed while having a constant water flux from the (presently) warm-based  
648 glacier, Slakbreen, which is juxtaposed and above the Slaknosa plateau. Regardless, the role of permafrost as a  
649 seal in highland areas is clearly more complex than in the valleys. Another mechanism that could prevent water  
650 from entering and freezing in the permafrost interval could be the early emplacement and trapping of gas.

651 Natural pathways through the cryospheric cap, even in areas of thick permafrost, are present in the form of  
652 pingos, springs, warm-based glaciers, and beneath the fjords. Ice maybe more prone to fracturing, particularly in  
653 shallow intervals where it is under little compression (Schulson, 2001). This may lead to fracture pathways



654 through the cryospheric cap although they likely self-heal through freezing water. At the Reindalen petroleum  
655 exploration, pingo holes are situated up-dip and probably represent a natural leak point for gas (Fig. 17).  
656 Elevated gas readings at 120 m in the wellbore likely represent a migration pathway at the base of permafrost  
657 toward the pingos. Similarly, gas shows at Kapp Laitone coincide with a potential migration pathway at the base of  
658 permafrost. The crestal point of this carrier bed is a short distance offshore (Fig. 10) which is also coincidental  
659 with the presence of pockmarks on the seafloor (Roy et al., 2015) where a potentially shallow permafrost tapers  
660 out.



661  
662 **Figure 17 – A seismic section intersecting the Reindalspasset wellbore, from Bælum and Braathen (2012). Deeper**  
663 **thermogenic gas likely migrates through the crests of the Billefjorden Fault Zone. Further shallow migration occurs**  
664 **through permeable Cretaceous stratigraphy and bypasses the permafrost seal through the pingo system to the west.**  
665 **The location of the seismic section is shown in Fig. 12.**

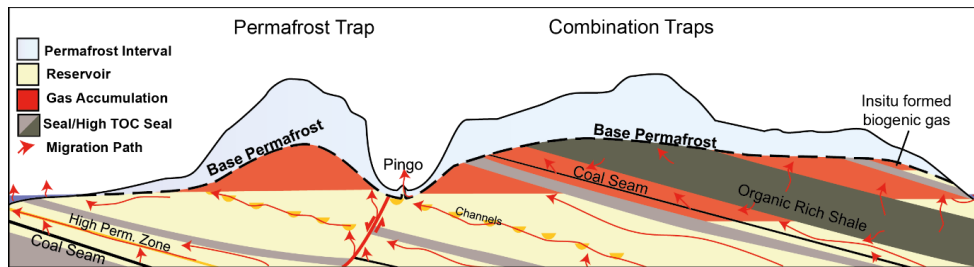
666

### 667 5.3 Permafrost Traps

668 In order for gas to accumulate beneath the permafrost a trap must be present. The undulating base of permafrost  
669 can form a trap and seal itself, or it may act as the top seal in combination with the underlying geology, these  
670 examples are shown in Fig. 18. In the former, traps may form beneath mountains if the interval is water  
671 saturated. This is because, although thicker, the base of permafrost is shallower than the surrounding valleys and  
672 leads to natural concave-down structures for buoyant gas accumulations. In valley settings where the base  
673 permafrost forms a synclinal structure it is more likely that accumulations are situated within combination traps.  
674 This is further supported by the fact the regional and local geology in Svalbard is rarely flat and contains  
675 multiple lithological seals and reservoirs. In these traps a combination of structural geology, lithology and  
676 permafrost properties contribute to developing hydrocarbon accumulations. This mechanism can be attributed to  
677 the gas accumulation in Adventdalen (Fig. 19). The combination of this combination trap type and the ice-  
678 saturated seals may explain why gas accumulations have been frequently encountered in valleys rather than



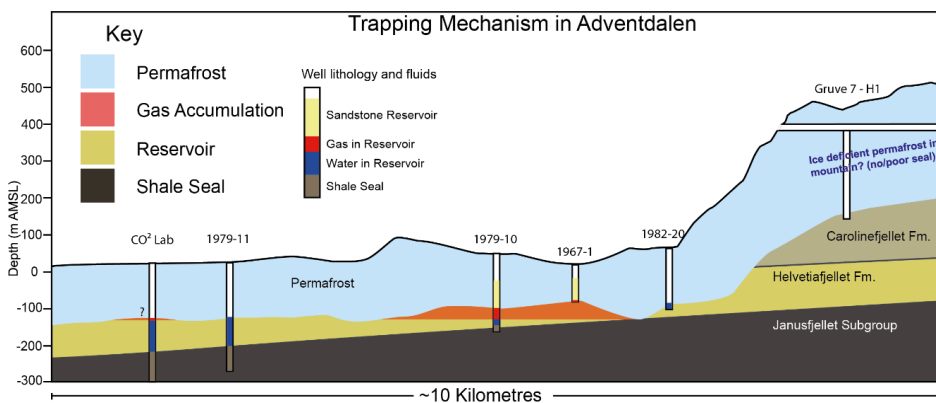
679 migrating and accumulating beneath shallower permafrost in highlands. Smaller accumulations, such as the one  
 680 encountered in Gipsdalen, may be restricted to localised undulations in the base-permafrost.



681

682 **Figure 18 – The different trapping mechanisms permafrost can provide. Undulations in the base permafrost alone**  
 683 **may form traps, which may be large under mountains if the permafrost seal is effective. Combination traps require**  
 684 **permafrost to contribute a lesser sealing surface area and appears to be the mechanism for trapping gas in**  
 685 **Adventdalen (Fig. 19).**

686 Gas trapped in hydrate form under the right thermobaric conditions is the exception to the previously discussed  
 687 trapping mechanisms. The gas sampled at Hopen is a strong candidate to originate from hydrates. The heavier  
 688 gas composition (Table 4) means it has a greater propensity to form hydrates at a given depth and temperature  
 689 (Fig. 9C). The permafrost zone is drier in mountainous areas then it will mean the hydrostatic pressures beneath  
 690 them are lower than presently assumed. Therefore, they may be slightly less favourable for the formation of  
 691 natural gas hydrates due to lower-than-expected pressures.



692

693 **Figure 19 – The potential combination-trapping style of the Adventdalen gas accumulation based on well**  
 694 **observations.**

695

## 696 5.4 Origins of gas

697 Gas originating from permafrost is typically attributed to a biogenic origin, primarily because thermogenic gas is  
 698 generated and migrates on much longer timescales. While biogenic gas is undoubtedly a contributor to sub-  
 699 permafrost gas in Svalbard (Hodson et al., 2019), thermogenic gas is also clearly a major contributor in several



700 locations (Ohm et al., 2019). In light of this, the lack of any accumulations or significant shows in the wells on  
701 Edgeøya is probably due to the lack of an underlying prolific source rock.

702 Approximately 60% of wells in the Barents Shelf offer hydrocarbon shows (Senger et al., 2020), indicating that  
703 the basin has at one point in the past been almost saturated with hydrocarbons. The large ultra-shallow  
704 discoveries like Wisting, containing relatively unbiodegraded oil, are evidence of more geologically recent  
705 hydrocarbon migration. ~~This recent migration is almost certainly driven by major recent uplift over the past  
706 thousands to hundreds of thousands of years (Henriksen et al., 2011).~~

707 Svalbard itself has undergone the greatest uplift of anywhere in the region, hence its existence as an archipelago.  
708 The numerous prolific source rocks mean Svalbard is unique from other Arctic areas. Recent uplift has enabled  
709 gas to escape directly from the source rocks or from deeper accumulations. The formation of permafrost has  
710 effectively added a last line of defence preventing this gas from escaping to the atmosphere.

711

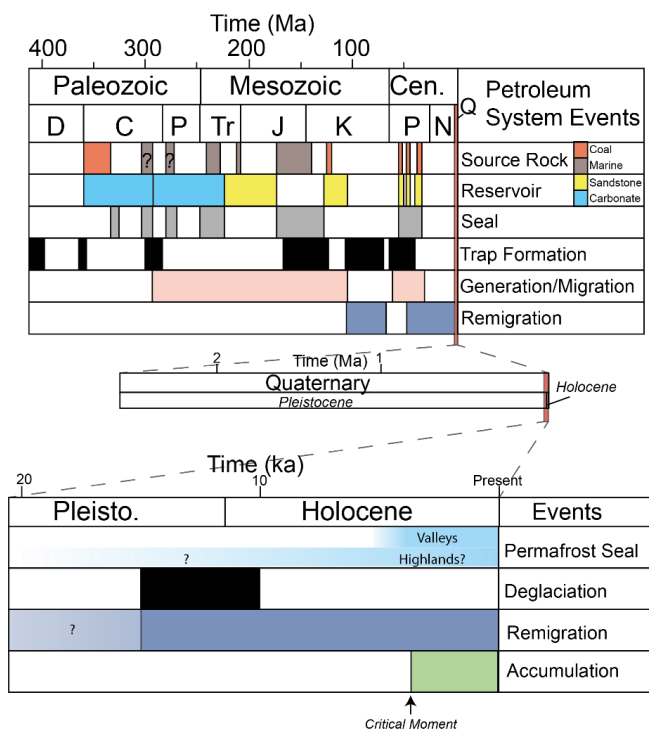
## 712 5.5 Timing and migration

713 Figure 20 is a petroleum systems chart with a focus on sub-permafrost accumulations in Svalbard. Clearly, all  
714 other elements of the petroleum system must be present prior to migration taking place. Here the timescales are  
715 binary with source, reservoirs and lithological seals forming tens or hundreds of millions of years ago and  
716 permafrost forming during the past few or tens of thousands of years. Therefore, the most critical elements in this  
717 system are the permafrost seal and gas migration.

718

719 The thermogenic gas must have been originated generated long before the formation of permafrost in the area  
720 because the source rocks of the area are no longer deep enough to generate hydrocarbons. Recent migration is  
721 almost certainly occurred during recent and ongoing uplift (Henriksen et al., 2011) due to repeated cycles of  
722 glacial loading and unloading (Ohm et al., 2008). This has been ongoing throughout the Pleistocene and predates  
723 permafrost formation. Therefore, the critical moment for most sub-permafrost gas accumulations in Svalbard is  
724 the timing of permafrost formation itself. The exception to this is in the extremely young moraine sediments in  
725 the case of Kapp Amsterdam, which also highlights ongoing gas migration.

726 Gas migration will occur through permeable intervals, typically at the crest of structures. Faults may aid the  
727 movement of gas from deeper structures, particularly during uplift and fault reactivation as appears to be the case  
728 at Reindalen (Fig. 17) which sits on the Billefjorden Fault Zone (Bælum and Braathen, 2012). The discovery of  
729 shale gas in Adventdalen (Ohm et al., 2019) also shows that source rocks still internally trap large amounts of  
730 gas. This gas will have migrated directly out of source rocks during uplift due to gas expansion and rock  
731 fracturing.



732

733 **Figure 20 - Petroleum systems chart for Svalbard. The upper part covers the important elements of the past 400**  
 734 **million years whereas the lower parts show the importance of the most recent events. The critical moment is the**  
 735 **timing of permafrost formation, which is also evidence that gas migration must also have been occurring recently, and**  
 736 **most likely ongoing today.**

737

### 738 5.6 Size, frequency and consequences of gas accumulations

739 Gas accumulations beneath permafrost appear to be a common occurrence in Svalbard and they show no  
 740 preference to stratigraphic age or geological setting. It is important to remember that none of the wells that  
 741 encountered sub-permafrost gas were actually looking for it, indeed most hydrocarbon exploration wells aim to  
 742 avoid such shallow gas accumulations (Ronen et al., 2012). In this study, of eighteen hydrocarbon wells in  
 743 Svalbard, eight show good evidence of permafrost (44%). Four of these permafrost bearing wells show moveable  
 744 gas accumulations at the base of permafrost (22% of all wells or 50% of permafrost bearing wells), three clearly  
 745 show no presence of an accumulation while one contains gas shows. Expanding this to all wells in this study, 18  
 746 show evidence of permafrost and 9 of these showing evidence of gas accumulations (50%), though the coal wells  
 747 for this study were obviously selected in areas of interest. This is an extremely high success rate for something  
 748 that was not being looked for, and thus highlights the likelihood that these gas accumulations are a very common  
 749 occurrence. For reference, the Barents Shelf has one of the highest technical success rates in the world at just  
 750 below 50% (Norwegian Petroleum Directorate, 2020) for prospects that have been specifically targeted using  
 751 advanced geological and geophysical methods.



752 As with conventional hydrocarbon accumulations, the size of sub-permafrost accumulations probably varies  
753 significantly. The accumulation in Adventdalen is relatively significant, but also of little economic interest; the  
754 1967-1 well produced in excess of 2.5 million cubic metres of gas between 1967 and 1975 (Snsk, 1981). Despite  
755 being of little economic interest, these accumulations may still provide an alternative and cleaner energy source  
756 than coal, which is presently used to generate power in Svalbard. Unfortunately the data are quite poor because  
757 the well was also periodically shut in over this time. Speculatively, if the convex-up shaped base permafrost  
758 below mountains acts as an effective trap then volumes may be even larger than the (relatively) better understood  
759 accumulations, in the valleys. Given the encountered overpressures in both water and gas bearing rocks it is fair  
760 to assume that the permafrost seal can withstand significant buoyancy pressures or large gas columns. It is more  
761 likely that the accumulations are regulated laterally by natural pathways through the permafrost at pingos, fjords  
762 or glaciers.

<b>Area of Hopen</b>	<b>46.12 km<sup>2</sup></b>
<b>Approximate thickness of hydrate stability zone</b>	600 m (This study)
<b>Net to Gross (sandstone)</b>	25% (Hynne, 2010)
<b>Average Porosity</b>	14% (Mørk, 2013)
<b>Volume as free gas</b>	968 Million Sm <sup>3</sup>
<b>If Hydrate</b>	154.963 Billion Cu. m.

763 **Table 6 – Estimation of gas volume under Hopen using properties from the stated publications. This assumes the**  
764 **stability zone is saturated to its base, which is highly dependent on the migration rate of gas. This may be somewhat**  
765 **unreasonable to assume but it is worth noting that the wells did monitor persistent gas influxes throughout the entire**  
766 **interval.**

767 Because the sub-permafrost accumulations are relatively shallow and under lower pressure, the gas will be much  
768 less dense, and thus voluminous, than conventional deeper accumulations. The exception to this is if the gas is in  
769 hydrate form where methane concentrations are some 160 times higher than in free gas form (Majorowicz and  
770 Hannigan, 2000). Table 6 shows the potential volumes of gas within the hydrate stability zone beneath Hopen  
771 using typical net to gross and reservoir properties for the De Geerdalen Formation (Mørk, 2013; Hynne, 2010).  
772 The calculations show volumes for both free gas, under atmospheric pressure and if it is in hydrate form.

773 Given the sparse data and bias in drilling locations it is impossible to be very quantitative with respect to the size  
774 and frequency of these accumulations. What is evident is that permafrost is acting as an ultimate seal to these  
775 accumulations, and that they are numerous, and, based on the only occurrence where flow was recorded, on the  
776 orders of million cubic metres.

777

## 778 5.7 Regional distribution

779 Based on the occurrences in Svalbard, the prerequisites for sub-permafrost gas to accumulate are, firstly, an  
780 impermeable (ice-saturated) permafrost layer, secondly, a source of gas and, finally, gas migration at a time after  
781 permafrost formation. Much of the Circum-Arctic shares a similar geological history with Svalbard. A major  
782 source of migrating gas in Svalbard is likely from the Mesozoic source rocks (Ohm et al., 2019), which can also



783 be found in the Russian and North American Arctic (Leith et al., 1993; Polyakova, 2015). Recent uplift caused  
784 by isostatic rebound has left fluids in the subsurface on the Barents and Svalbard out of pressure equilibrium and  
785 driving present-day migration (Birchall et al., 2020). Svalbard shares its Pleistocene glacial history with the  
786 Circum-Arctic (Batchelor et al., 2019) so it is not unreasonable to expect sub-permafrost gas accumulations to be  
787 regionally widespread. Indeed, gas emanating from zones of permafrost is well-documented onshore and  
788 offshore in the Russian Arctic, particularly in hydrocarbon provinces (Chuvilin et al., 2020 and references  
789 therein) and as natural gas hydrates (Yakushev & Chuvilin, 2000).

790

## 791 **6 Conclusion**

792 Although gas at the base of permafrost has been encountered frequently during more than fifty years of drilling  
793 in Svalbard, it has not been studied or widely recognised until now. In this study we have provided a synthesis of  
794 historical and modern observations and their implications. Our key findings are:

- 795 • Gas accumulations trapped at the base of permafrost occur throughout the archipelago in several  
796 stratigraphic intervals.
- 797 • The gas accumulations are evidence for ongoing hydrocarbon migration
- 798 • Gas encountered in wellbores on Hopen is compositionally heavier and likely within the gas hydrate  
799 stability zone
- 800 • Permafrost is a good seal in valleys but appears to possess permeable intervals in highland areas
- 801 • Groundwater flow below permafrost is much greater than previously documented
- 802 • There is evidence of relatively thick coastal permafrost, particularly in eastern Svalbard

803 ~~Because methane is a potent greenhouse gas and the Arctic is warming faster than anywhere else on Earth (Lind~~  
804 ~~et al., 2018), the release of sub-permafrost gas accumulations in Svalbard may contribute a positive climatic~~  
805 ~~feedback effect. Shallow gas associated with permafrost has been documented throughout much of the Circum-~~  
806 ~~Arctic (Nielsen et al., 2014; Minshull et al., 2020; Hodson et al., 2020; Chuvilin et al., 2020). Because Svalbard~~  
807 ~~shares much of its geological and glacial history with the Circum-Arctic it seems likely that the gas~~  
808 ~~accumulations we document in Svalbard are more widespread.~~

809

## 810 **Acknowledgements**

811 This research is funded by the Research Centre for Arctic Petroleum Exploration (ARCEX) partners and the  
812 Research Council of Norway (grant number 228107), CLIMAGAS (grant number 284764) and the Norwegian



813 CCS Research Centre (grant number 257579). We sincerely appreciate access to Store Norske Spitsbergen  
814 Kulkompani's vast internal archives and to the data from the Longyearbyen CO<sub>2</sub> lab project ([http://co2-](http://co2-ccs.unis.no)  
815 [ccs.unis.no](http://co2-ccs.unis.no)). We also thank Sarah Strand for fruitful discussions on permafrost dynamics.



## 816 References

- 817 Aagaard, K., Foldvik, A., and Hillman, S.: The West Spitsbergen Current: disposition and water mass  
818 transformation, *Journal of Geophysical Research: Oceans*, 92, 3778-3784,  
819 <https://doi.org/10.1029/JC092iC04p03778>, 1987.
- 820 Abay, T., Karlsen, D., Lerch, B., Olaussen, S., Pedersen, J., and Backer-Owe, K.: Migrated petroleum in  
821 outcropping Mesozoic sedimentary rocks in Spitsbergen: Organic geochemical characterization and  
822 implications for regional exploration, *Journal of Petroleum Geology*, 40, 5-36,  
823 <https://doi.org/10.1111/jpg.12662>, 2017.
- 824 Anell, I. M., Braathen, A., and Olaussen, S.: The Triassic–Early Jurassic of the northern Barents Shelf: a  
825 regional understanding of the Longyearbyen CO<sub>2</sub> reservoir, *Norsk Geologisk Tidsskrift*, 94, 83-98,  
826 2014.
- 827 Anthony, K. M. W., Anthony, P., Grosse, G., and Chanton, J.: Geologic methane seeps along  
828 boundaries of Arctic permafrost thaw and melting glaciers, *Nature Geoscience*, 5, 419-426,  
829 <https://doi.org/10.1038/ngeo1480>, 2012.
- 830 Bælum, K. and Braathen, A.: Along-strike changes in fault array and rift basin geometry of the  
831 Carboniferous Billefjorden Trough, Svalbard, Norway, *Tectonophysics*, 546, 38-55,  
832 <https://doi.org/10.1016/j.tecto.2012.04.009>, 2012.
- 833 Batchelor, C. L., Margold, M., Krapp, M., Murton, D. K., Dalton, A. S., Gibbard, P. L., Stokes, C. R.,  
834 Murton, J. B., and Manica, A.: The configuration of Northern Hemisphere ice sheets through the  
835 Quaternary, *Nature Communications*, 10, 1-10, <https://doi.org/10.1038/s41467-019-11601-2>, 2019.
- 836 Beka, T. I., Senger, K., Autio, U. A., Smirnov, M., and Birkelund, Y.: Integrated electromagnetic data  
837 investigation of a Mesozoic CO<sub>2</sub> storage target reservoir-cap-rock succession, Svalbard, *Journal of*  
838 *Applied Geophysics*, 136, 417-430, <https://doi.org/10.1016/j.jappgeo.2016.11.021>, 2017.
- 839 Betlem, P., Senger, K., and Hodson, A.: 3D thermobaric modelling of the gas hydrate stability zone  
840 onshore central Spitsbergen, Arctic Norway, *Marine and Petroleum Geology*, 100, 246-262,  
841 <https://doi.org/10.1016/j.marpetgeo.2018.10.050>, 2019.
- 842 Betlem, P., Midttømme, K., Jochmann, M., Senger, K., and Olaussen, S.: Geothermal Gradients on  
843 Svalbard, Arctic Norway, First EAGE/IGA/DGMK Joint Workshop on Deep Geothermal Energy, cp-577-  
844 00017,
- 845 Bily, C. and Dick, J.: Naturally occurring gas hydrates in the Mackenzie Delta, NWT, *Bulletin of*  
846 *Canadian Petroleum Geology*, 22, 340-352, <https://doi.org/10.35767/gscpgbull.22.3.340>, 1974.
- 847 Birchall, T., Senger, K., Hornum, M., Olaussen, S., and Braathen, A.: Underpressure in the northern  
848 Barents shelf: Causes and implications for hydrocarbon exploration, *AAPG Bulletin*, 38,  
849 <https://doi.org/10.1306/02272019146>, 2020.
- 850 Birkenmajer, K., Nagy, J., and Dallmann, W. K.: Geological Map Svalbard 1:100,000. Markhambreen,  
851 Spitsbergen, Norsk Polarinstitut, Tromsø, 1992.
- 852 Blinova, M., Inge Faleide, J., Gabrielsen, R. H., and Mjelde, R.: Seafloor expression and shallow  
853 structure of a fold-and-thrust system, Isfjorden, west Spitsbergen, *Polar Research*, 31, 11209,  
854 <https://doi.org/10.3402/polar.v31i0.11209>, 2012.
- 855 Boucher, O., Friedlingstein, P., Collins, B., and Shine, K. P.: The indirect global warming potential and  
856 global temperature change potential due to methane oxidation, *Environmental Research Letters*, 4,  
857 044007, 2009.
- 858 Braathen, A., Bælum, K., Maher Jr, H., and Buckley, S. J.: Growth of extensional faults and folds during  
859 deposition of an evaporite-dominated half-graben basin; the Carboniferous Billefjorden Trough,  
860 Svalbard, *Norwegian Journal of Geology*, 91, 137, 2012.
- 861 Christiansen, H. H., French, H. M., and Humlum, O.: Permafrost in the Gruve-7 mine, Adventdalen,  
862 Svalbard, *Norsk Geografisk Tidsskrift-Norwegian Journal of Geography*, 59, 109-115,  
863 <https://doi.org/10.1080/00291950510020592>, 2005.
- 864 Christiansen, H. H., Etzelmüller, B., Isaksen, K., Juliussen, H., Farbrøt, H., Humlum, O., Johansson, M.,  
865 Ingeman-Nielsen, T., Kristensen, L., and Hjort, J.: The thermal state of permafrost in the Nordic area



- 866 during the International Polar Year 2007–2009, *Permafrost and Periglacial Processes*, 21, 156-181,  
867 <https://doi.org/10.1002/ppp.687>, 2010.
- 868 Chuvilin, E., Yakushev, V. S., and Perlova, E.: Gas and possible gas hydrates in the permafrost of  
869 Bovanenkovo Gas Field, Yamal Peninsula, west Siberia, *Polarforschung*, 68, 215-219, 2000.
- 870 Chuvilin, E., Ekimova, V., Davletshina, D., Sokolova, N., and Bukhanov, B.: Evidence of Gas Emissions  
871 from Permafrost in the Russian Arctic, *Geosciences*, 10, 383,  
872 <https://doi.org/10.3390/geosciences10100383>, 2020.
- 873 Collett, T. S., Lee, M. W., Agena, W. F., Miller, J. J., Lewis, K. A., Zyrianova, M. V., Boswell, R., and Inks,  
874 T. L.: Permafrost-associated natural gas hydrate occurrences on the Alaska North Slope, *Marine and  
875 Petroleum Geology*, 28, 279-294, <https://doi.org/10.1016/j.marpetgeo.2009.12.001>, 2011.
- 876 Dallmann, W. K., Elvevold, S., Gerland, S., Hormes, A., Majka, J., Ottemöller, L., Pavlova, O., and  
877 Sander, G.: *Geoscience atlas of Svalbard*, 2nd Edition, Norsk Polarinstitut, Tromsø, Norway 2015.
- 878 Dimakis, P., Braathen, B. I., Faleide, J. I., Elverhøi, A., and Gudlaugsson, S. T.: Cenozoic erosion and the  
879 preglacial uplift of the Svalbard–Barents Sea region, *Tectonophysics*, 300, 311-327,  
880 [https://doi.org/10.1016/S0040-1951\(98\)00245-5](https://doi.org/10.1016/S0040-1951(98)00245-5), 1998.
- 881 Divine, D. V. and Dick, C.: Historical variability of sea ice edge position in the Nordic Seas, *Journal of  
882 Geophysical Research: Oceans*, 111, <https://doi.org/10.1029/2004JC002851>, 2006.
- 883 Dörr, N., Lisker, F., Jochmann, M., Rainer, T., Schlegel, A., Schubert, K., and Spiegel, C.: Subsidence,  
884 rapid inversion, and slow erosion of the Central Tertiary Basin of Svalbard: Evidence from the thermal  
885 evolution and basin modeling, in: *Circum-Arctic Structural Events: Tectonic Evolution of the Arctic  
886 Margins and Trans-Arctic Links with Adjacent Orogens*, edited by: Piepjohn, K., Strauss, J. V., Lutz, R.,  
887 and McClelland, W. C., The Geological Society of America, Boulder, Colorado, 169-188, 2018.
- 888 Dypvik, H. and Zakharov, V.: Fine-grained epicontinental Arctic sedimentation–mineralogy and  
889 geochemistry of shales from the Late Jurassic-Early Cretaceous transition, *Norwegian Journal of  
890 Geology/Norsk Geologisk Forening*, 92, 65-87, 2012.
- 891 Faleide, J. I., Solheim, A., Fiedler, A., Hjelstuen, B. O., Andersen, E. S., and Vanneste, K.: Late Cenozoic  
892 evolution of the western Barents Sea-Svalbard continental margin, *Global and Planetary Change*, 12,  
893 53-74, [https://doi.org/10.1016/0921-8181\(95\)00012-7](https://doi.org/10.1016/0921-8181(95)00012-7), 1996.
- 894 Gasser, D.: *The Caledonides of Greenland, Svalbard and other Arctic areas: status of research and  
895 open questions*, Geological Society, London, Special Publications, 390, 93-129,  
896 <https://doi.org/10.1144/SP390.17>, 2014.
- 897 Gilbert, G. L., O'Neill, H. B., Nemeč, W., Thiel, C., Christiansen, H. H., and Buylaert, J. P.: Late  
898 Quaternary sedimentation and permafrost development in a Svalbard fjord-valley, *Norwegian high  
899 Arctic, Sedimentology*, 65, 2531-2558, <https://doi.org/10.1111/sed.12476>, 2018.
- 900 Grundvåg, S.-A., Jelby, M. E., Śliwińska, K. K., Nøhr-Hansen, H., Aadland, T., Sandvik, S. E., Tennvassås,  
901 I., Engen, T., and Olausen, S.: Sedimentology and palynology of the Lower Cretaceous succession of  
902 central Spitsbergen: integration of subsurface and outcrop data, *Norwegian Journal of Geology*, 99,  
903 253-284, <https://doi.org/10.17850/njg006>, 2019.
- 904 Harada, K. and Yoshikawa, K.: Permafrost age and thickness near Adventfjorden, Spitsbergen, *Polar  
905 Geography*, 20, 267-281, <https://doi.org/10.1080/10889379609377607>, 1996.
- 906 Henriksen, E., Bjørnseth, H., Hals, T., Heide, T., Kiryukhina, T., Kløvjan, O., Larssen, G., Ryseth, A.,  
907 Rønning, K., and Sollid, K.: Uplift and erosion of the greater Barents Sea: impact on prospectivity and  
908 petroleum systems, Geological Society, London, *Memoirs*, 35, 271-281,  
909 <https://doi.org/10.1144/M35.17>, 2011.
- 910 Hodson, A. J., Nowak, A., Holmlund, E., Redeker, K. R., Turchyn, A. V., and Christiansen, H. H.:  
911 Seasonal dynamics of Methane and Carbon Dioxide evasion from an open system pingo: Lagoon  
912 Pingo, Svalbard, *Frontiers in Earth Science*, 30, 1-12, <https://doi.org/10.3389/feart.2019.00030>, 2019.
- 913 Hodson, A. J., Nowak, A., Senger, K., Redeker, K., Christiansen, H. H., Jessen, S., Hornum, M. T.,  
914 Betlem, P., Thornton, S. F., and Turchyn, A. V.: Open system pingos as hotspots for sub-permafrost  
915 methane emission in Svalbard, *The Cryosphere Discussions*, 1-21, 2020.



- 916 Hornum, M. T., Hodson, A. J., Jessen, S., Bense, V., and Senger, K.: Numerical modelling of permafrost  
917 spring discharge and open-system pingo formation induced by basal permafrost aggradation, The  
918 Cryosphere Discussions, 1-36, <https://doi.org/10.5194/tc-14-4627-2020>, 2020.
- 919 Howarth, R. W., Santoro, R., and Ingraffea, A.: Methane and the greenhouse-gas footprint of natural  
920 gas from shale formations, *Climatic change*, 106, 679, <https://doi.org/10.1007/s10584-011-0061-5>,  
921 2011.
- 922 Humlum, O.: Holocene permafrost aggradation in Svalbard, Geological Society, London, Special  
923 Publications, 242, 119-129, <https://doi.org/10.1144/GSL.SP.2005.242.01.11>, 2005.
- 924 Humlum, O., Instanes, A., and Sollid, J. L.: Permafrost in Svalbard: a review of research history,  
925 climatic background and engineering challenges, *Polar research*, 22, 191-215, 2003.
- 926 Huq, F., Smalley, P. C., Mørkved, P. T., Johansen, I., Yarushina, V., and Johansen, H.: The  
927 Longyearbyen CO<sub>2</sub> Lab: Fluid communication in reservoir and caprock, *International Journal of*  
928 *Greenhouse Gas Control*, 63, 59-76, <https://doi.org/10.1016/j.ijggc.2017.05.005>, 2017.
- 929 Hynne, I. B.: Depositional environment on eastern Svalbard and central Spitsbergen during Carnian  
930 time (Late Triassic): A sedimentological investigation of the De Geerdalen Formation, Institutt for  
931 geovitenskap og petroleum, Norwegian University of Science and Technology, Trondheim, 2010.
- 932 Isaksen, K., Mühl, D. V., Gubler, H., Kohl, T., and Sollid, J. L.: Ground surface-temperature  
933 reconstruction based on data from a deep borehole in permafrost at Janssonhaugen, Svalbard,  
934 *Annals of Glaciology*, 31, 287-294, <https://doi.org/10.3189/172756400781820291>, 2000.
- 935 Jochmann, M. M., Augland, L. E., Lenz, O., Bieg, G., Haugen, T., Grundvåg, S. A., Jelby, M. E.,  
936 Midtkandal, I., Dolezych, M., and Hjálmarsdóttir, H. R.: Sylfjellet: a new outcrop of the Paleogene Van  
937 Mijenfjorden Group in Svalbard, arktos, 1-22, 2019.
- 938 Johansen, T. A., Digranes, P., van Schaack, M., and Lønne, I.: Seismic mapping and modeling of near-  
939 surface sediments in polar areas, *Geophysics*, 68, 566-573, <https://doi.org/10.1190/1.1567226>, 2003.
- 940 Juliussen, H., Jochmann, M., and Christiansen, H. H.: High-mountain permafrost temperature  
941 monitoring in central Svalbard; implications for Arctic coal mining., Third European Conference on  
942 Permafrost; EUCOP III, Svalbard, 06/13/2010,
- 943 Kamath, A., Godbole, S., Ostermann, R., and Collett, T.: Evaluation of the stability of gas hydrates in  
944 northern Alaska, *Cold Regions Science and Technology*, 14, 107-119, [https://doi.org/10.1016/0165-  
945 232X\(87\)90026-7](https://doi.org/10.1016/0165-232X(87)90026-7), 1987.
- 946 Keating, K., Binley, A., Bense, V., Van Dam, R. L., and Christiansen, H. H.: Combined geophysical  
947 measurements provide evidence for unfrozen water in permafrost in the adventdalen valley in  
948 Svalbard, *Geophysical Research Letters*, 45, 7606-7614, <https://doi.org/10.1029/2017GL076508>,  
949 2018.
- 950 Klausen, T. G., Nyberg, B., and Helland-Hansen, W.: The largest delta plain in Earth's history, *Geology*,  
951 47, 470-474, <https://doi.org/10.1130/G45507.1>, 2019.
- 952 Knoblauch, C., Beer, C., Liebner, S., Grigoriev, M. N., and Pfeiffer, E.-M.: Methane production as key  
953 to the greenhouse gas budget of thawing permafrost, *Nature Climate Change*, 8, 309-312,  
954 <https://doi.org/10.1038/s41558-018-0095-z>, 2018.
- 955 Koevoets, M. J., Hammer, Ø., Olaussen, S., Senger, K., and Smelror, M.: Integrating subsurface and  
956 outcrop data of the middle Jurassic to Lower Cretaceous Agardhfjellet formation in central  
957 Spitsbergen, *Norwegian Journal of Geology*, 98, 1-34, 2018.
- 958 Kristensen, L., Benn, D. I., Hormes, A., and Ottesen, D.: Mud aprons in front of Svalbard surge  
959 moraines: evidence of subglacial deforming layers or proglacial glaciotectonics?, *Geomorphology*,  
960 111, 206-221, 2009.
- 961 Landvik, J., Mangerud, J., and Salvigsen, O.: Glacial history and permafrost in the Svalbard area,  
962 *Proceedings of the 5th International Conference on Permafrost*, 194-198,
- 963 Landvik, J. Y., Brook, E. J., Gualtieri, L., Raisbeck, G., Salvigsen, O., and Yiou, F. o.: Northwest Svalbard  
964 during the last glaciation: Ice-free areas existed, *Geology*, 31, 905-908, 2003.
- 965 Landvik, J. Y., Bondevik, S., Elverhøi, A., Fjeldskaar, W., Mangerud, J., Salvigsen, O., Siegert, M. J.,  
966 Svendsen, J.-I., and Vorren, T. O.: The last glacial maximum of Svalbard and the Barents Sea area: ice



- 967 sheet extent and configuration, *Quaternary Science Reviews*, 17, 43-75,  
968 [https://doi.org/10.1016/S0277-3791\(97\)00066-8](https://doi.org/10.1016/S0277-3791(97)00066-8), 1998.
- 969 Lasabuda, A., Laberg, J. S., Knutsen, S.-M., and Safronova, P.: Cenozoic tectonostratigraphy and pre-  
970 glacial erosion: A mass-balance study of the northwestern Barents Sea margin, Norwegian Arctic,  
971 *Journal of Geodynamics*, 119, 149-166, <https://doi.org/10.1016/j.jog.2018.03.004>, 2018.
- 972 Lashof, D. A. and Ahuja, D. R.: Relative contributions of greenhouse gas emissions to global warming,  
973 *Nature*, 344, 529-531, <https://doi.org/10.1038/344529a0>, 1990.
- 974 Leith, T., Weiss, H., Mørk, A., Elvebakk, G., Embry, A., Brooks, P., Stewart, K., Pchelina, T., Bro, E., and  
975 Verba, M.: Mesozoic hydrocarbon source-rocks of the Arctic region, in: Norwegian petroleum society  
976 special publications, Elsevier, 1-25, <https://doi.org/10.1016/B978-0-444-88943-0.50006-X>, 1993.
- 977 Leythaeuser, D., Mackenzie, A., Schaefer, R. G., and Bjorøy, M.: A novel approach for recognition and  
978 quantification of hydrocarbon migration effects in shale-sandstone sequences, *AAPG bulletin*, 68,  
979 196-219, <https://doi.org/10.1306/AD4609FE-16F7-11D7-8645000102C1865D>, 1984.
- 980 Lind, S., Ingvaldsen, R. B., and Furevik, T.: Arctic warming hotspot in the northern Barents Sea linked  
981 to declining sea-ice import, *Nature climate change*, 8, 634-639, 2018.
- 982 Lord, G. S., Solvi, K. H., Ask, M., Mørk, A., Hounslow, M. W., and Paterson, N. W.: The hopen member:  
983 a new member of the Triassic De Geerdalen Formation, Svalbard, Norwegian Petroleum Directorate  
984 Bulletin, 11, 81-96, 2014.
- 985 Lyutkevich, E. M.: Geology of Tertiary Coals of Spitzbergen, Isfjord Region, *Truds Arkticheskogo*  
986 *Instituta*, 76, 7-24, 1937.
- 987 Magnabosco, C., Braathen, A., and Ogata, K.: Permeability model of tight reservoir sandstones  
988 combining core-plug and Miniper analysis of drillcore; Longyearbyen CO2 Lab, Svalbard, Norwegian  
989 journal of geology, 94, 189-200, 2014.
- 990 Magoon, L. and Dow, W.: Mapping the Petroleum System--An Investigative Technique to Explore the  
991 Hydrocarbon Fluid System, *AAPG Memoir*, 73, 53-68, 2000.
- 992 Majewski, W. and Zajaczkowski, M.: Benthic foraminifera in Adventfjorden, Svalbard: Last 50 years of  
993 local hydrographic changes, *The Journal of Foraminiferal Research*, 37, 107-124,  
994 <https://doi.org/10.2113/gsjfr.37.2.107>, 2007.
- 995 Majorowicz, J. and Hannigan, P.: Stability Zone of Natural Gas Hydrates in a Permafrost-Bearing  
996 Region of the Beaufort—Mackenzie Basin: Study of a Feasible Energy Source1 (Geological Survey of  
997 Canada Contribution No. 1999275), *Natural resources research*, 9, 3-26,  
998 <https://doi.org/10.1023/A:1010105628952>, 2000.
- 999 Makogon, Y. and Omelchenko, R.: Commercial gas production from Messoyakha deposit in hydrate  
1000 conditions, *Journal of Natural Gas Science and Engineering*, 11, 1-6,  
1001 <https://doi.org/10.1016/j.jngse.2012.08.002>, 2013.
- 1002 Marshall, C., Large, D. J., Meredith, W., Snape, C. E., Uguna, C., Spiro, B. F., Orheim, A., Jochmann, M.,  
1003 Mokogwu, I., and Wang, Y.: Geochemistry and petrology of Palaeocene coals from Spitsbergen—Part  
1004 1: Oil potential and depositional environment, *International Journal of Coal Geology*, 143, 22-33,  
1005 <https://doi.org/10.1016/j.coal.2015.03.006>, 2015.
- 1006 Marum, D. M., Afonso, M. D., and Ochoa, B. B.: Optimization of the Gas-Extraction Process in a New  
1007 Mud-Logging System, *SPE Drilling & Completion*, 35, 13, <https://doi.org/10.2118/198909-PA>, 2019.
- 1008 Masoudi, R. and Tohidi, B.: Estimating the hydrate stability zone in the presence of salts and/or  
1009 organic inhibitors using water partial pressure, *Journal of Petroleum Science and Engineering*, 46, 23-  
1010 36, <https://doi.org/10.1016/j.petrol.2004.10.002>, 2005.
- 1011 Michelsen, J. K. and Khorasani, G. K.: A regional study on coals from Svalbard; organic facies, maturity  
1012 and thermal history, *Bulletin de la Société Géologique de France*, 162, 385-397, 1991.
- 1013 Minshull, T. A., Marín-Moreno, H., Betlem, P., Bialas, J., Buenz, S., Burwicz, E., Cameselle, A. L., Cifci,  
1014 G., Giustiniani, M., and Hillman, J. I.: Hydrate occurrence in Europe: A review of available evidence,  
1015 *Marine and Petroleum Geology*, 111, 735-764, <https://doi.org/10.1016/j.marpetgeo.2019.08.014>,  
1016 2020.
- 1017 Mørk, M. B. E.: Compositional Variations and Provenance of Triassic Sandstones from the Barents  
1018 Shelf, *Journal of Sedimentary Research*, 69, 690-710, <https://doi.org/10.2110/jsr.69.690>, 1999.



- 1019 Mørk, M. B. E.: Diagenesis and quartz cement distribution of low-permeability Upper Triassic–Middle  
1020 Jurassic reservoir sandstones, Longyearbyen CO<sub>2</sub> lab well site in Svalbard, Norway, AAPG Bulletin, 97,  
1021 577-596, <https://doi.org/10.1306/10031211193>, 2013.
- 1022 Nielsen, T., Laier, T., Kuijpers, A., Rasmussen, T. L., Mikkelsen, N. E., and Nørgård-Pedersen, N.: Fluid  
1023 flow and methane occurrences in the Disko Bugt area offshore West Greenland: indications for gas  
1024 hydrates?, *Geo-Marine Letters*, 34, 511-523, <https://doi.org/10.1007/s00367-014-0382-2>, 2014.
- 1025 Norsk Hydro: Final Well Report - 7816/12-1, HarstadSVA021, 122, 1991.
- 1026 Norsk Polar Navigasjon A/S: Geological Report - Tromsøbreen No. 1, Stabekk, Oslo, 1977a.
- 1027 Norsk Polar Navigasjon A/S: Final Drilling Report - Tromsøbreen No. 1, Stabekk, Oslo, 1977b.
- 1028 Norske Fina A/S: Final Drilling Report - Well Hopen No. 1, Stabekk, Oslo, 1971a.
- 1029 Norske Fina A/S: Geological Report - Well Hopen No. 1, Stabekk, Oslo, 1971b.
- 1030 Norske Fina A/S: Geological Report - Well: Plurdalen No. 1, Norske Fina, 1972a.
- 1031 Norske Fina A/S: Final Drilling Report - Well: Plurdalen No.1, Norske Fina, 71, 1972b.
- 1032 Norske Fina A/S: Geological Report - Well Hopen No. 2, Stabekk, Oslo, 1973a.
- 1033 Norske Fina A/S: Final Drilling Report - Well Hopen No. 2, 1973b.
- 1034 Exploration Activity: <https://www.norskpetroleum.no/en/exploration/exploration-activity/>, last  
1035 access: 20/07/2020.
- 1036 Norwegian Polar Institute: Svalbardkartet, Norwegian Polar Institute, Norsk Polarinstitutt WebGIS,  
1037 Tromsø, 10.21334/npolar.2014.645336c7, 2015.
- 1038 Nøttvedt, A., Cecchi, M., Gjelberg, J., Kristensen, S., Lønøy, A., Rasmussen, A., Rasmussen, E., Skott,  
1039 P., and Van Veen, P.: Svalbard-Barents Sea correlation: a short review, in: *Norwegian Petroleum*  
1040 *Society Special Publications*, Elsevier, 363-375, 1993.
- 1041 Ohm, S., Larsen, L., Olausen, S., Senger, K., Birchall, T., Demchuk, T., Hodson, A., Johansen, I.,  
1042 Titlestad, G. O., Karlsen, D. A., and Braathen, A.: Discovery of shale gas in organic-rich Jurassic  
1043 successions, Adventdalen, Central Spitsbergen, Norway, *Norwegian Journal of Geology*, 99, 28,  
1044 <https://dx.doi.org/10.17850/njg007>, 2019.
- 1045 Ohm, S. E., Karlsen, D. A., and Austin, T.: Geochemically driven exploration models in uplifted areas:  
1046 Examples from the Norwegian Barents Sea, AAPG Bulletin, 92, 1191-1223,  
1047 <https://doi.org/10.1306/06180808028>, 2008.
- 1048 Olausen, S., Senger, K., Braathen, A., Grundvåg, S. A., and Mørk, A.: You learn as long as you drill;  
1049 research synthesis from the Longyearbyen CO<sub>2</sub> Laboratory, Svalbard, Norway, *Norwegian Journal of*  
1050 *Geology*, 99, 157-187, <https://dx.doi.org/10.17850/njg008>, 2019.
- 1051 Olausen, S., Larssen, G. B., Helland-Hansen, W., Johannessen, E. P., Nøttvedt, A., Riis, F., Rismyhr, B.,  
1052 Smelror, M., and Worsley, D.: Mesozoic strata of Kong Karls Land, Svalbard, Norway; a link to the  
1053 northern Barents Sea basins and platforms, *Norwegian Journal of Geology*, 98, 1-69, 2018.
- 1054 Osterkamp, T. and Payne, M.: Estimates of permafrost thickness from well logs in northern Alaska,  
1055 *Cold Regions Science and Technology*, 5, 13-27, [https://doi.org/10.1016/0165-232X\(81\)90037-9](https://doi.org/10.1016/0165-232X(81)90037-9),  
1056 1981.
- 1057 Piepjohn, K.: The Svalbardian-Ellesmerian deformation of the Old Red Sandstone and the pre-  
1058 Devonian basement in NW Spitsbergen (Svalbard), *Geological Society, London, Special Publications*,  
1059 180, 585-601, <https://doi.org/10.1144/GSL.SP.2000.180.01.31>, 2000.
- 1060 Polargas Prospektering KB: Geological Report - Tromsøbreen No. 2, Stabekk, Oslo, 1988.
- 1061 Polyakova, I.: Petroleum source rocks of the Arctic region, *Lithology and Mineral Resources*, 50, 26-  
1062 49, <https://doi.org/10.1134/S002449021406008X>, 2015.
- 1063 Rachelewicz, G. and Szczuciński, W.: Changes in thermal structure of permafrost active layer in a dry  
1064 polar climate, Petuniabukta, Svalbard, *Polish Polar Research*, 29, 261-278, 2008.
- 1065 Rismyhr, B., Bjærke, T., Olausen, S., Mulrooney, M., and Senger, K.: Facies, palynostratigraphy and  
1066 sequence stratigraphy of the Wilhelmøya Subgroup (Upper Triassic–Middle Jurassic) in western  
1067 central Spitsbergen, Svalbard, *Norwegian Journal of Geology*, 99, 35-64,  
1068 <https://dx.doi.org/10/17850/njg001>, 2019.



- 1069 Ronen, S., Rokkan, A., Bouraly, R., Valsvik, G., Larson, L., Ostensvig, E., Paillet, J., Dynia, A., Matlosz,  
1070 A., and Brown, S.: Imaging shallow gas drilling hazards under three Forties oil field platforms using  
1071 ocean-bottom nodes, *The Leading Edge*, 31, 465-469, <https://doi.org/10.1190/tle31040465.1>, 2012.
- 1072 Roy, S., Hovland, M., Noormets, R., and Olausen, S.: Seepage in Isfjorden and its tributary fjords,  
1073 West Spitsbergen, *Marine Geology*, 363, 146-159, <http://dx.doi.org/10.1016/j.margeo.2015.02.003>,  
1074 2015.
- 1075 Schmitt, D., Welz, M., and Rokosh, C.: High-resolution seismic imaging over thick permafrost at the  
1076 2002 Mallik drill site, *Geological Survey of Canada Bulletin*, 585, 125, 2005.
- 1077 Schulson, E. M.: Brittle failure of ice, *Engineering fracture mechanics*, 68, 1839-1887,  
1078 [https://doi.org/10.1016/S0013-7944\(01\)00037-6](https://doi.org/10.1016/S0013-7944(01)00037-6), 2001.
- 1079 Senger, K., Tveranger, J., Ogata, K., Braathen, A., and Planke, S.: Late Mesozoic magmatism in  
1080 Svalbard: A review, *Earth-Science Reviews*, 139, 123-144,  
1081 <https://doi.org/10.1016/j.earscirev.2014.09.002>, 2014.
- 1082 Senger, K., Birchall, T., Betlem, P., Ogata, K., Ohm, S., Olausen, S., and Paulsen, R. S.: Resistivity of  
1083 reservoir sandstones and organic rich shales on the Barents Shelf: Implications for interpreting CSEM  
1084 data, *Geoscience Frontiers*, 64, <https://doi.org/10.1016/j.gsf.2020.08.007>, 2020.
- 1085 Senger, K., Brugmans, P., Grundvåg, S.-A., Jochmann, M. M., Nøttvedt, A., Olausen, S., Skotte, A.,  
1086 and Smyrak-Sikora, A.: Petroleum, coal and research drilling onshore Svalbard: a historical  
1087 perspective, *Norwegian Journal of Geology*, 99, 30, <https://doi.org/10.17850/njg99-3-1>, 2019.
- 1088 Skorobogatov, V. A., Yakushev, V. S., and Chuvilin, E. M.: Sources of natural gas within permafrost;  
1089 North-West Siberia, *Permafrost Proceedings Seventh International Conference, Collection Nordicana*,  
1090 1001-1007,
- 1091 Sloan Jr, E. D., Koh, C. A., and Koh, C.: *Clathrate hydrates of natural gases*, CRC press 2007.
- 1092 Smyrak-Sikora, A., Johannessen, E. P., Olausen, S., Sandal, G., and Braathen, A.: Sedimentary  
1093 architecture during Carboniferous rift initiation—the arid Billefjorden Trough, Svalbard, *Journal of the*  
1094 *Geological Society*, 176, 225-252, <https://doi.org/10.1144/jgs2018-100>, 2019.
- 1095 SNSK: Report SN1979\_002, Longyearbyen, 14, 1979.
- 1096 SNSK: Drawing Nr. 14204-3; Borhullslogg 79/11 Endalen, Longyearbyen, 1980.
- 1097 SNSK: Report SN1981\_008, Longyearbyen, 52, 1981.
- 1098 SNSK: Report SN1982\_004, Longyearbyen, 14, 1982a.
- 1099 SNSK: Report SN1982\_005, Longyearbyen, 14, 1982b.
- 1100 SNSK: Report SN1986\_001, Longyearbyen, 14, 1986.
- 1101 SNSK: Report SN1991.04, Longyearbyen, 14, 1991.
- 1102 SNSK: Report - Kapp Laila - 1, Longyearbyen, 110, 1994.
- 1103 SNSK: BH 19-2011 Drilling Report, Longyearbyen, 14, 2011a.
- 1104 SNSK: BH 18-2011 Drilling Report, Longyearbyen, 14, 2011b.
- 1105 SNSK: BH 16-2011 Drilling Report, Longyearbyen, 14, 2011c.
- 1106 SNSK: BH 14-2011 Drilling Report, Longyearbyen, 14, 2011d.
- 1107 SNSK: BH 7-2013 Drilling Report, Longyearbyen, 14, 2013a.
- 1108 SNSK: BH 10-2013 Drilling Report, Longyearbyen, 14, 2013b.
- 1109 SNSK: BH 6-2013 Drilling Report, Longyearbyen, 14, 2013c.
- 1110 SNSK: BH 8-2014 Drilling Report, Longyearbyen, 14, 2014.
- 1111 Steel, R., Dalland, A., Kalgraff, K., and Larsen, V.: The Central Tertiary Basin of Spitsbergen:  
1112 sedimentary development of a sheared-margin basin, *AAPG Memoir*, 7, 647-664, 1981.
- 1113 Steel, R. J. and Worsley, D.: Svalbard's post-Caledonian strata - an atlas of sedimentational patterns  
1114 and paleogeographic evolution, in: *Petroleum Geology of the North European Margin*, edited by:  
1115 Spencer, A. M., Graham & Trotman, London, 109-135, [https://doi.org/10.1007/978-94-009-5626-1\\_9](https://doi.org/10.1007/978-94-009-5626-1_9),  
1116 1984.
- 1117 Strand, S. M., Christiansen, H. H., Johansson, M., Åkerman, J., and Humlum, O.: Active layer  
1118 thickening and controls on interannual variability in the Nordic Arctic compared to the circum-Arctic,  
1119 *Permafrost and Periglacial Processes*, DOI:10.1002/ppp.2088, in press.
- 1120 Total Marine Norsk: Final Well Report - Raddalen I, 1972.



- 1121 Uguna, J. O., Carr, A. D., Marshall, C., Large, D. J., Meredith, W., Jochmann, M., Snape, C. E., Vane, C.  
1122 H., Jensen, M. A., and Olaussen, S.: Improving spatial predictability of petroleum resources within the  
1123 Central Tertiary Basin, Spitsbergen: a geochemical and petrographic study of coals from the eastern  
1124 and western coalfields, *International Journal of Coal Geology*, 179, 278-294,  
1125 <https://doi.org/10.1016/j.coal.2017.06.007>, 2017.
- 1126 van Pelt, W. J., Kohler, J., Liston, G., Hagen, J. O., Luks, B., Reijmer, C., and Pohjola, V. A.: Multidecadal  
1127 climate and seasonal snow conditions in Svalbard, *Journal of Geophysical Research: Earth Surface*,  
1128 121, 2100-2117, <https://doi.org/10.1002/2016JF003999>, 2016.
- 1129 Verba, M.: Kollektornye svoystva porod osadochnogo chekhla arhipelaga Shpitsbergen [Sedimentary  
1130 cover reservoir of Svalbard archipelago], *Neftegazovaya Geologiya. Teoriya i Praktika*, 8, 1-45, 2013.
- 1131 Vonk, J. E. and Gustafsson, Ö.: Permafrost-carbon complexities, *Nature Geoscience*, 6, 675-676,  
1132 <https://doi.org/10.1038/ngeo1937>, 2013.
- 1133 Vrielink, H. J., Bradford, J. S., Basarab, L., and Ubaru, C. C.: Successful application of casing-while-  
1134 drilling technology in a Canadian arctic permafrost application, IADC/SPE Drilling Conference,  
1135 <https://doi.org/10.2118/111806-MS>,
- 1136 Westermann, S., Wollschläger, U., and Boike, J.: Monitoring of active layer dynamics at a permafrost  
1137 site on Svalbard using multi-channel ground-penetrating radar, *The Cryosphere*, 4, 475-487,  
1138 <https://doi.org/10.5194/tc-4-475-2010>, 2010.
- 1139 Yakushev, V. and Chuvilin, E.: Natural gas and gas hydrate accumulations within permafrost in Russia,  
1140 *Cold regions science and technology*, 31, 189-197, [https://doi.org/10.1016/S0165-232X\(00\)00012-4](https://doi.org/10.1016/S0165-232X(00)00012-4),  
1141 2000.
- 1142
- 1143



1144 **Author Contribution**

1145 **Thomas Birchall:** Conceptualisation, methodology, validation, investigation, data curation, writing – original  
1146 draft, writing – review and editing, visualisation, project administration.

1147 **Malte Jochmann:** Conceptualization, Validation, Investigation, Resources, Data Curation, writing – reviewing

1148 **Peter Betlem:** Methodology, Software, Validation, writing – reviewing

1149 **Kim Senger:** Conceptualization, methodology, validation, resources, writing – reviewing, supervision

1150 **Andrew Hodson:** Validation, writing – reviewing, supervision

1151 **Snorre Olaussen:** Validation, writing – reviewing, supervision

1152

1153

1154 **Competing Interests**

1155 The authors have no known competing interests.

1156

1157

1158 **Data Availability**

1159 The historical nature of the data and reports means they are available in hard-copy only. Reports referenced in  
1160 this article are proprietary to their respective companies.

1161 For permafrost and hydrate stability modelling herein, the methodology is detailed in the following publication:

1162 <https://doi.org/10.1016/j.marpetgeo.2018.10.050>

1163